የኢፌዴሪ የቴክኒክና ሙያ ስልጠና ኢንስቲትዩት
FDRE TECHNICAL & VOCATIONAL TRAINING INSTITUTE

TECHNICAL AND VOCATIONAL TRAINING INSTITUTION (TVTI)

School of Graduate Studies

FACULTY OF ELECTRICAL AND ELECTRONICS TECHNOLOGY AND INFORMATION AND COMMUNICATION TECHNOLOGY

(DEPARTMENT OF ELECTRONICS AND COMMUNICATION TECHNOLOGY MANAGEMENT)

THESIS ON: DESIGN DOUBLE LAYER AERIAL WITH LENS FOR MILLIMETER WAVE IMAGE DETECTION SYSTEMS

Thesis for the Partial Fulfillment of Master of Science (MSc.) in Electronics and communication Technology Management

By,

Ehtinat Amisalu (TTMR/091/16)

Supervisor,

Yoseph Kefyalew**, PhD**

June 2025

Addis Ababa, Ethiopia

የኢፌዴሪ የቴክኒክና ሙያ ስልጠና ኢንስቲትዩት
FDRE TECHNICAL & VOCATIONAL TRAINING INSTITUTE

DESIGN DOUBLE LAYER AERIAL WITH LENS FOR MILLIMETER WAVE IMAGE DETECTION SYSTEMS

A Thesis submitted to:

TECHNICAL AND VOCATIONAL TRAINING INSTITUTE (TVTI)

FACULTY OF ELECTRICAL AND ELECTRONICS TECHNOLOGY AND INFORMATION AND COMMUNICATION TECHNOLOGY (DEP'T OF ELECTRICAL AND ELECTRONICS TECHNOLOGY)

IN PARTIAL FULFILLMENT FOR THE

MASTER OF SCIENCE IN ELECTRONICS AND COMMUNICATION TECHNOLOGY MANAGEMENT

By,

Ehtinat Amisalu (TTMR/091/16)

Supervisor,

Yoseph Kefyalew, PhD

Jan 2026

Addis Ababa, Ethiopia

DECLARATIONS

I hereby declare that this thesis paper is my original work, has not been presented for a degree in this or any other university, and all necessary sources of materials used for the thesis have been duly acknowledged.

Name: _______________

Signature: _________________________

Place: Addis Ababa

Date of Submission: _________________

This thesis has been submitted for examination with my approval as a TVTI advisor.

Advisor Name: Yosef Kefyalew

Signature -----------------------------------

Date: 03/09/2026 ----------------------------------

ACKNOWLEDGEMENT

To begin with, I am a very grateful person to my Almighty God who has bestowed upon me the health, strength, and perseverance which is needed to accomplish this thesis. I would like to claim my unapprehensive gratitude to my advisor Dr. Yosef Kefyalew. direction, patience and knowledge. His tips, motivation and advice are precious. strong and constant encouragement played a key role in the development of this work and its actualization. I also owe a lot to my family, friends and colleagues as they are always there. direct and indirect encouragement, understanding and support, which contributes much. helped in the achievement of this study research.

TABLE OF CONTENTS

ABSTRACT

There has been significant interest in millimeter-wave systems used in detection of concealed images. security, medical and industrial fields because of their ability to detect concealed items with. minimal penetration loss. Current antenna designs, i.e. single-layer patch antennas. Slot designs, and APSAs have low gain, small bandwidth, low directivity, and are generally low gain. restrained detection range, and hence less image resolution and fidelity. To overcome these challenges, this work is a patch antenna of circular form on the double-layer with an inbuilt lens, optimized at 24.411 GHz - the best millimeter-wave radio frequency to use in imaging. The High Frequency Structure Simulator (HFSS) was used to develop and simulate design. utilizing multi-layer layouts and lenses in order to increase radiation effectiveness and beam. focusing. Performance tests were taken to be of importance with regard to gain, directivity, and reflection. coefficient (S11), voltage standing wave ratio (VSWR) and bandwidth which were subsequently correlated. to useful imaging parameters like spatial resolution and range of detection. Simulation results report that the proposed antenna has a total gain of 30.2 dB, directivity of 30.14 dB, -16.933 dB reflection coefficient, a VSWR of 2.4 and a wide bandwidth of 35.933 GHz. This facilitates imaging operation at high fidelity with spatial resolution of 2–3mm and detection limits of 510m, significantly better than single-layer or lens-free designs that have been reported in the literature. This the proposed research introduces a vacuum in the literature, as it offers usable high-performance framework. millimeter-wave concealed imaging, that lens-assisted double-layer antennas can. at the same time improve gain, bandwidth and image quality. The results were well grounded. to develop long-range and high-resolution millimeter-wave imaging systems in the future.

Keywords: Millimeter-wave, Concealed Image Detection, Double-layer Circular Patch Antenna. Lens-Assisted antenna, HFSS simulation, high gain antenna, broadband imaging, spatial resolution.

LIST OF TABLES

LIST OF FIGURES

LIST OF ABBREVIATION AND ACRONYM.

GHz…………………………………………… Giga Hertz

Ohm/sq…………………………………………Ohm per square

MMW………………………………………… millimeter Wave.

dBi…………………………………………… Decibel

MPAA………………………………………… Micro strip Patch Array Antenna

FSS…………………………………………… Frequency Selective Surfaces

MPA……………………………………………Micro strip Patch Antenna.

mm……………………………………………...millimeter

W……………………………………………… Watt

CST……………………………………………...Computer Simulation Technology

G bps…………………………………………… Giga bytes per second.

ISM band………………………………………Industrial, scientific, and medical radio band

AFTSA…………………………………………Antipodal Fermi tapered slot antenna

RHCPA………………………………………… Right-hand circularly polarized antenna

PET……………………………………………… piezoelectric transducer

E-Plane…………………………………Electric field/determine the polarization of Radio waves.

H-Plane…………………………………………H-field/Direction of maximum radiation.

EBG……………………………………………Electromagnetic Band Gap.

SGH……………………………………………standard gain horn

MCAFTSA-SC probe……………………. Multi Corrugated Antipodal Fermi tapered slot antenna

S11/S22………………………………………… Simulation and measured return loss

CHATPTER ONE

INTRODUCTIONS

1.1. Background of the study

According to Institute of Electrical Electronics Engineering (IEEE) Standard letter designation for Radar frequency bands, Millimeter-Wave (MMW) is classified as technology operating in the frequency band of 30 GHz to 300GHz, which corresponds to wavelengths range of 1-mm to 10-mm. The band belongs to Extremely high frequency (EHF). Thus, this frequency band is widely used in security applications for the detection of concealed weapons and non-destructive testing for assessment of deterioration of concrete structure. Infrared waves do not provide these unique properties of millimeter waves. Visible or infrared imaging system is weak visibility of image during poor weather condition and X-ray technology imaging system hazardous to human body during scanning the target. Millimeter-wave imaging offers safe, non-ionizing radiation with strong penetration through common dielectric materials such as clothing, plastics, and wood. In addition, it maintains reliable performance under adverse environmental conditions, including rain, fog, and dust, making it well suited for concealed object detection applications. Making it safe for human body scanning applications. For these reasons, this band offers a remarkable opportunity to perform surveillance. Today, millimeter-wave wireless technology is a very attractive field of research, particularly in the unlicensed 24 GHz band. Designing a high-performance millimeter-wave antenna is a significant challenge in millimeter-wave image detection applications. The significant requirements of 24GHz antenna for image detection purpose are high gain, highly directive beam, low side lobe level and narrow beam width. Therefore, the main objective of this study is to investigate and design an improved millimeter-wave antenna for image detection applications. This thesis focuses on the design of a double-layer circular patch antenna integrated with a dielectric lens at 24 GHz, with the expectation of significantly improving antenna gain, directivity, spatial resolution, and detection range compared to conventional single-layer designs.

1.2. Problem Statement

Millimeter-wave concealed image detection systems are increasingly important for security, medical, and industrial applications due to their ability to detect hidden objects with high penetration capability and minimal interference. Existing antenna designs including single-layer patch antennas, Q-slot antennas, APSAs, and some multi-layer configurations frequently exhibit low gain, restricted directivity, narrow bandwidth, and less-than-optimal radiation efficiency. These shortcomings limit spatial resolution, image clarity, and detection range, resulting in coarser imaging, lower signal-to-noise ratios, and reduced effectiveness for practical concealed object detection. Moreover, there is a notable absence of comprehensive design strategies that combine multilayer patch structures with lens-assisted radiation enhancement to simultaneously boost gain, bandwidth, and imaging performance. Overcoming these challenges is critical for developing high-performance millimeter-wave imaging systems capable of achieving high-resolution, long-range detection of concealed objects.

1.3.Objective

1.3.1. General Objective

1.3.2. Design Better patch antenna at 24GHz Improved Double Layer Circular patch antenna with lens to achieve imaging

Specific Objectives

- Design and develop a lens-integrated, double-layer circular patch antenna. optimized to operate at 24.411⁻ millimeter-wave concealed image detection.
- Perform extensive electromagnetic simulations in HFSS to determine important antenna. Characteristics, such gain and directivity as well as reflection coefficient (S11), VSWR & operational bandwidth.
- Determine the effect of the performance of the antenna on imaging quality measures including spatial. resolution, detection range and signal-to-noise ratio.

- Comparative analysis of the proposed design and single-layer and earlier reported antenna. setups to bring out better gains, directivity, bandwidth and generally. undetected imaging efficacy.

1.4.Significance of the Study

This thesis makes a significant contribution to the advancement of millimeter-wave (mmWave) imaging technologies through the development of a novel double-layer antenna system. The proposed design enhances signal strength, beam control, and image clarity, which are critical for precision-driven applications such as security scanning, automotive sensing, and medical diagnostics. By integrating a multi-layer antenna structure with a lens, the system achieves improved efficiency and stability, while the lens focuses electromagnetic waves to deliver higher-

The compact and versatile design enables seamless integration into portable and lightweight devices, as well as sophisticated electronic systems. Furthermore, its robust performance under conditions of limited visibility or electromagnetic interference ensures practical applicability in real-world scenarios. Overall, this research advances high-performance mmWave sensor technology, with promising applications in emerging fields including 6G communications, autonomous navigation, and intelligent surveillance infrastructures.

1.5.Scope of the Study

This study focuses on the design, simulation and performance evaluation of a two-layer. often referred to as millimeter-wave (mmWave) imaging systems, an antenna in combination with a dielectric lens. The study focuses on improving enhancing gain, directivity and resolution of the image in the antenna under the high. frequency conditions of mmWave applications. The field of application is limited to the appraisal. simulation, but not actual fabrication, of the electromagnetic properties of the antenna. or implementation of a real-time system. Applications that may be dealt with in the simulation.

Organizations of the Thesis

This thesis has a structure of six chapters, each of which addresses one of the main aspects of the research on. designing a dielectric lens plus a millimeter-wave (mmWave) antenna design based on a two-layer antenna design. imaging systems:

Chapter 1: Introduction

In this chapter, the background of the research is presented, the problem statement is given, and the outlines of the. purposes, and describes the importance and the breadth of the study. It determines the impetus to designing more improved antennas to fit in mmWave imaging.

Chapter 2: Literature Review

The extensive survey of the past literature in the field of millimeter-wave antennas, lens integration, and This chapter presents imaging systems. It recognizes gaps in the research, assesses existing design. arguments, and justifies why the proposed two-layer antenna set-up is necessitated.

Chapter 3: System Design and Methodology

This chapter elaborates on the conceptual design of the double-layer antenna and how they are coupled with a. dielectric lens. Themes covered are the choice of the material, tools of the simulation and a step by step. approach to the modeling and analysis of the electromagnetic performance of the antenna.

Chapter 4: Simulation and Performance Analysis

The simulation environment and the most important performance indicators including gain, beamwidth, return loss and. The patterns of radiation are introduced here. Conventional comparisons with results are made quantitatively. designs of the antennas in order to draw attention to the superiorities of the proposed two-layer construction.

Chapter 5: Results and Discussion

Simulation outcomes are interpreted in the context of mmWave imaging applications. This chapter discusses how the proposed antenna design enhances image resolution and detection accuracy, addresses design limitations, and suggests areas for future refinement.

Chapter 6: Conclusion and Future Work

The final chapter summarizes the main findings, highlights the contributions of the research, and outlines prospective future directions, including hardware prototyping, real-world testing, and applications in advanced mmWave imaging systems.

CHAPTER TWO

LITERATURE REVIEWS.

2.1.Introduction to the Millimeter-Wave Antenna Technology.

The millimeter-wave (mmWave) band at 24 GHz is a part of a relatively new area of research that has been targeted by researchers as the potential area of high-speed wireless communications and imaging uses. Although this band is of high frequency given that it enables compact antenna design, it has certain challenges including higher propagation losses and limited depth of penetration. Various research works have addressed the various design techniques to address these setbacks and enhance the important performance metrics, such as gain, bandwidth, efficiency, and signal transparency [1].

2.2.Improvements in Patch Antenna Arrangements and Uses.

Various designs of millimeter-wave (mmWave) antennas that have been investigated to improve gain, bandwidth, and imaging have been studied previously. In one of the studies, the optically transparent 4X 2 patch arrays of patch arrays were studied and manufactured on fused quartz substrates. These arrays employed metallic meshes in micro meter scale covered with silver to ensure the electrical conductivity and still reach greater than 80 percent optical transparency in the visible range. Despite the structural and aesthetic advantages of transparency, the maximum gain achieved at 15.6 0.6 -1 reached 13.6 dBi which is a little less than the 15.6 dBi achievable with opaque arrays demonstrating the trade -off between antenna gain and optical visibility [2].

The other research was on the topic of the compact dual-band circular patch antennas under the 57.24-65.88GHz frequency range working as duplexers. Feeding the patch on both sides at right angles stimulated two orthogonal resonant modes. The patch size optimization and impedance transformation through transmission lines yielded nearly the same results in the simulated and measured return loss and pattern of radiation. Two-layer electromagnetically coupled patches have also been used to make high-gain mmWave antennas. The designs facilitated wide impedance matching, broad bandwidths in the vicinity of 8GHz and peak gain of 18.7 dbi in massive quantities by using stacked in the form of circles interlocked with substrates such as Rogers RO3003 and Taconic FR-27, thus proving to be useful in high-data-rate communication systems [3].

Microstrip patch antennas are also used because they are small in size, lightweight and easy to integrate. Nevertheless, they have low bandwidth and an average gain that may need improvement measures. The first would be to place frequency-selective surfaces (FSSs) both above and beneath the patch array, which would dramatically enhance gain, bandwidth, and return loss, which is confirmed by simulations of CST Microwave Studio [4]. Some of these variations include stripline-fed circular patches on low-loss Duroid substrates, which have been used in defense applications with high gain and low surface wave loss, with return loss of up to -24.77 -1 dB at 24 GHz by optimizing the feedline offset [5].

To achieve body-centric communication, a slotted Q-patch antenna made on FR4 has been shown to have both a 12GHz or higher impedance bandwidth, and a 8.62dBi peak gain. Even though the closer the proximity to the human body, the lower the radiation efficiency, performance was sufficient to be used on the short-range, high-data-rate applications [6].

Periodic antennas Periodic antennas Periodic antennas with aperiodic geometries and low number of elements have been suggested to provide low-cost coverage of the 24-GHz band. On low-loss substrates like Rogers RT5880, these designs had bandwidths of 20.66% and gains of 11.8Go, which allowed them to be used in wideband applications with compact, linear-phase characteristics [7]. Triangular and slot-based microstrip patch shape-optimized antennas have been invented to be integrated in 5G with a gain of up to 8 dBi and good return loss, at a small footprint, which is suitable in portable or embedded devices in the 61.93 GHz band [8].

To realize wider mmWave applications, high gain, low-cost U-slot-fed patch antennas on thin low permittivity substrates such as Rogers RT/Duroid 5880 provided two paths, bandwidth of 11.6%, and gains exceeding 8dBi, and proved to be the solution to short range unlicensed communications [9].

There have been also major breakthroughs in mmWave imaging systems of detecting concealed objects. Tapered slot antennas and circular patch-fed dielectric lens antennas are found to be high-resolution images, reaching gains of about 20dBi and 3GHz bandwidth. Other advancements are beam-steering arrays that are phase shifted and corrugated lens geometry which enables better directional control and side lobes reduction. These designs were experimentally validated as effective in detection of hidden threats like weapons or contraband in the real-life situation [10]. 3 Dielectric Lens Integration and Beam-Steering Techniques.

This part is a review of the recent developments in the mmWave (wideband) lens antenna designs. One of these is the construction of an automated design process that builds a library of matched unit cells and consists of impedance-matching sections and phase-delaying cores. This allows aperture efficiencies of 31-72% at a 2.9:1 bandwidth, and thus is such a design to 5G mmWave frequencies [1].

Maximization of gain in mmWave lens antennas using phase-center analysis has been used. This was done by optimal placement of the lens in relation to the antenna element, which improved its gain by approximately 25 percent compared to traditional designs [2].

A third design uses a UV-LIGA fabrication and NOA73 material to design a dual-focus mmWave radar system antenna, and 22 0 -dBi gain at 100 GHz antenna is obtained in compact radar applications [3].

An antenna array antenna-fed lens has been designed to synthesize near-field plane waves at mmWave frequencies with a reduced propagation range but with the same amplitude and phase [4]. Gradient-index lens antennas have likewise been developed to support small mmWave MIMO apparatus, offering beam-steering to 44C, at low loss and low expense to mobile purposes [5].

Dual-polarized flat Luneburg lenses on multilayer PCBs realized gains of 16.818.8 dBi and beam-scanning angles of up to -25 o C, with applicability to mmWave applications [6]. Systems that utilize intelligent reflecting surface (IRS) to combine lens antenna arrays have been proposed to combine transmit and reflection beamforming to optimize energy efficiency [7].

Micromachining of flat silicon mesh arrays of lens arrays in mmWave and sub-mmWave astronomy have been developed and coupled with planar antenna to make optically active detectors [8].

In the case of wind profile radar, the beam directions can be adjusted with the use of lens antennas with reconfigurable beams and beam-switching circuits integrated in the antennas [9].

The choice of materials has been demonstrated to have a strong influence on the level of beam scanning in the automotive radar that uses two lenses, which give high broadside directivity with minimal scan loss [10].

A 3-D near-field mmWave lens antenna based synthetic aperture radar (SAR) system with antenna pattern compensation to minimize grating lobes and sidelobes is applied to improve image resolution and accuracy of detection [11]. Microstrip arrays of antennas that use dielectric lenses provide the highest gains of 32 dBi at 77 GHz and are able to scan narrow beams over a broad angle [12].

Recent advances have seen the 3D-printed conformal meta-lenses with multiple beam-shaping capabilities, low-profile broadband, circularly polarized mmWave capabilities to augment sensing performance [13]. Compact antenna test ranges (CATR) based on lenses have been developed to measure at mmWave frequencies over-the-air with multiple angles of arrival represented in order to properly model the scenarios of wireless propagation [14].

All in all, those developments show that lens-integrated mmWave antennas have made great strides in terms of gain, bandwidth, beam-steering, and imaging of 5G communications and automotive radar, as well as in remote sensing and astronomy [15].

2.3. literature Summary

Table 2.1 Literature Summary

Ref	Year	Application	Antenna Types	Frequency	Bandwidth	Gain	V SWR	Gap
1	2016	Optical Transparent	Optical Transparent MSA	24GHz	30GHz	15.65 dB		Low Gain
2	2017	Duplexer	Dual band path antenna	24GHz	2.61 GHz	9.3 dB		Low gain and bandwidth
3	2016	Communicator	Multi-layer path	24GHz	8 GHz	12dBi 18, 7 dbi		Low Gain
4	2016	N/A	RMSPA	24GHz	0.625 GHz		1.67 dB	Complex
5	2017	Defense applications		24GHz	32GHz	7.499 dB		Low Gain
6	2021	Body centric communication	Q-slot antenna	24GHz	12.11 GHz	8.62 dB	1.5 dB	Narrow bandwidth and gain
7	2019	Broad Band high gain antenna.	5G communication	24GHz	20.66%	11.8 dB		Low Gain

8	2017	5G Communication	Triangular with slot.	24GHz	28GHz	8 dB		Low Gain
9	2016	Instant and applications	Printed U slotted.	24GHz	11.6%	8.2 dB		Narrow Bandwidth and Gain
10	2015	Imaging.	APSA	24GHz	32GHz	20 dB	< 3dB	Low Gain

2.4.Literature Summary Discussion

The table provides a comparative analysis of various microstrip antennas operating at 24 GHz, outlining their configurations, applications, and key performance metrics. One early design (2016) focused on optically transparent microstrip antennas suitable for scenarios requiring visibility through the antenna surface. While this design achieved a gain of 15.65 dB, it remained lower than conventional opaque antennas, illustrating the trade-off between optical transparency and electrical performance.

In 2017, a dual-band patch antenna was developed for duplexer applications. The design provided a moderate gain of 9.3 dB with a 2.61 GHz bandwidth, but its limited gain and narrow bandwidth constrained its use in high-speed communication systems. Another 2016 multilayer patch antenna aimed to enhance general communication performance, achieving gains of 12 dBi and 18.7 dBi over an 8 GHz bandwidth. While improved, the gain was still considered modest for advanced mmWave applications. A circular microstrip patch antenna (CMSPA) from the same year, however, exhibited a very narrow bandwidth of 0.625 GHz and low gain of 1.67 dB, limiting its suitability for broadband 24 GHz systems.

For defense applications, a 2017 circular patch fed via a stripline achieved a gain of 7.5 dB. Although functional, it was insufficient for long-range or high-resolution imaging. In 2021, a Q-slot antenna designed for body-centric communications provided a wide 12.11 GHz bandwidth with 8.62 dBi gain, but performance declined near the human body due to reduced radiation efficiency.

For 5G networks, a 2019 broadband antenna delivered 11.8 dB gain with a 20.66% bandwidth, offering a practical solution for wideband applications but still underperforming relative to other high-frequency designs. A 2017 triangular-slot patch for compact 5G devices achieved 8 dB gain but faced challenges in reaching higher gain levels. Similarly, a 2016 printed U-slot antenna provided 8.2 dB gain and 11.6% bandwidth, balancing cost-effectiveness with moderate performance.

Finally, a 2015 antipodal Fermi tapered slot antenna (AFTSA) for imaging systems achieved a peak gain of 20 dB and return loss below 3 dB, marking it as the most promising design in terms of combined bandwidth and gain, particularly for high-resolution applications.

Overall, while these designs demonstrate targeted innovations, most struggle to simultaneously achieve high gain and wide bandwidth at 24 GHz. This underscores a key challenge in millimeter-wave antenna engineering, where miniaturization, fabrication complexity, and material selection critically influence performance.

CHAPTER THREE

METHODOLOGY, THEORETICAL BACKGROUND AND METHOD OF ANALYSIS

3.1.Methodology Flow Chart

The study follows a structured approach, progressing from theoretical analysis to initial design development, and culminating in a fully optimized lens-integrated antenna system.

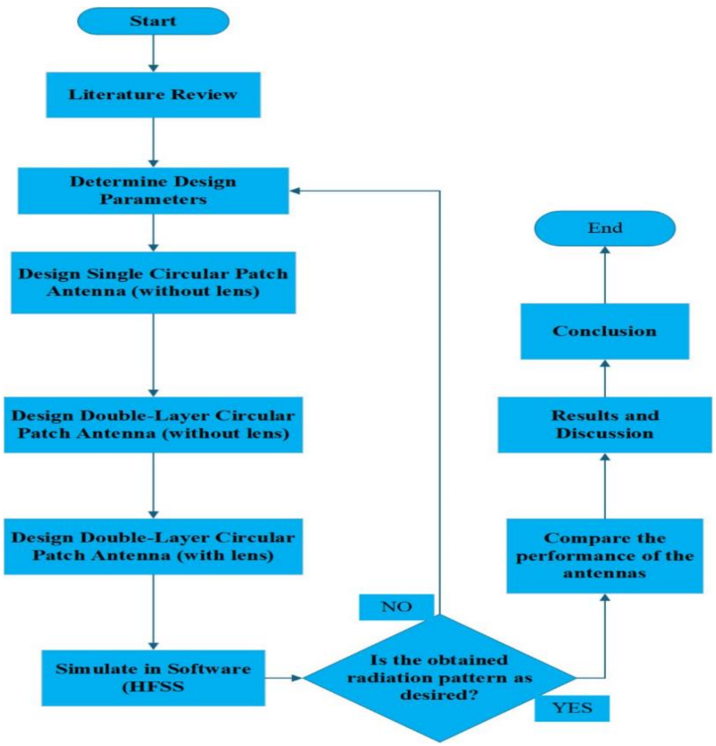

Figure 1 Methodology Flow Charts

3.2.Methodology Flow Chart Discussion.

- Start: This phase is an actual commencement of the research, which will entail defining the core problem, formulating research questions, as well as setting clear study objectives.
- Literature Review: Ten related studies were reviewed in details to identify the gaps in knowledge, trace the design trends through the history, and define the highest levels of performance use in previous research.
- Deflection of Design Parameters: Design variables and methods of analysis to be employed towards the development of the antenna are specified such as the substrate to use, frequency of operation and the mathematical models to be applied in assessing the antenna performance.
- Single-Layer Circular Patch Antenna Design (No Lens): The first step towards an antenna design is the creation of an antenna based on a single radiating circular patch. This design is a substitute to evaluate the improvement made in later designs.
- Double-Layer Circular Patch Antenna Design (Without Lens): To enhance performance indices, e.g., impedance bandwidth and gain, two-layer stacked dielectric antenna model is constructed, which has a better performance than the one-layer baseline.
- Double-layer Circular Patch Antenna Design (With Lens): The last design will use a dielectric lens to the antenna of the two layers to focus the radiated beam. This is a major advancement in gain and directivity and the general resolution of imaging.
- Simulation Modeling: The design of antenna is simulated on professional electromagnetic computer applications like CST Microwave Studio or HFSS. The results of the simulation give numerical values depending on the design parameters that were set earlier.
- Decision Point: Determine whether the design is up to the acceptable performance measures.
- Yes: Continue with the prediction of the imaging capabilities of the system.
- No: Go back to design parameter stage and refine the variables and optimize the performance.
- Imaging Performance Prediction: Digital Signal Processing (DSP) is used to extract the results of the simulation. The theoretical models are the estimates of the imaging potential and spatial resolution of the system.

- Performance Evaluation: Comparative analysis of the performance of the newly designed antenna against literature review results is to be done in order to validate the improvements as well as to make sure that the design is effective.
- Results Analysis and Discussion: The analysis and discussion of the data of the simulation are performed which covers the radiation patterns and the influence of the dielectric lens on the performance of the antennas.
- Conclusion and Future Directions: The conclusion of the research is summarized, with its major contributions mentioned, and recommendations given related to future research in millimeter-wave imaging and the development of high-resolution antennas.

3.3.Theoretical Background

This part gives the theoretical basis of millimeter-wave (mmWave) antennas to use in the 5G communication network, the discussion of feeding mechanisms, and the main antenna parameters that can be used in the applications of high-resolution concealed images detection.

3.3.1. Millimeter wave Band

The millimeter-wave (mmWave) spectrum lies in the genre of extremely high-frequency (EHF) and is 300 GHz to 30 GHz, or, expressed differently, 30 GHz to 300 GHz, as defined by the IEEE Standard for Radar Frequency Bands (2002 update of IEEE Standard 521-1984). The wavelengths within this spectrum go down to 1 mm and 10 mm and that is why the band is referred to as the millimeter-wave. Basically, the electromagnetic waves that are sent and received within this range are of wavelengths of millimeters.

The mmWave frequency is between the super high-frequency (SHF) range, and the far-infrared/terahertz range, which provides a total spectrum width of about 270 GHz. The basic principle of waves is that longer wavelengths are associated with a higher level of frequency. Thus, mmWave signals have extremely high frequencies and, accordingly, small wavelengths, which allow peculiarities of transmission.

The benefits of millimeter waves include; it is possible to design small antennas, it can survive large bandwidths and very high speeds of data transmission is achieved. They also have short propagation ranges and poor penetration through solid barriers however. Although these properties have a restrictive effect in other situations, they may also be used to improve the security and reliability of communication in the short-range scenario. mmWave technology was initially used in military and defense systems but has been used in civilian and scientific applications more frequently. The most important ones are the Internet of Things (IoT) devices, biomedical imaging, security screening, the detection of hidden objects, and interferometric radar. The Federal Communications Commission (FCC) expanded these possibilities in 2001 by designating an unlicensed band from 57 GHz to 64 GHz within the ISM (Industrial, Scientific, and Medical) spectrum. This allocation, particularly around the 24 GHz band, has promoted both academic research and commercial use of mmWave systems.

3.3.2. Millimeter Wave Antenna

Millimeter-wave (mmWave) antennas are specifically designed to operate within this spectrum. A wide variety of antenna types fall under this category, including Yagi–Uda antennas, hybrid antennas, stacked configurations, bow-tie antennas, circular patch antennas, and tapered slot antennas.

For millimeter-wave imaging and scanning systems, end-fire antennas are generally preferred over broadside types. This is because end-fire antennas provide higher gain, greater sensitivity, and improved target detection capability. Among these, tapered slot antennas (TSAs) are widely regarded as the most suitable option for mmWave imaging applications. Their advantages include a low-profile design, high radiation efficiency, symmetric radiation in both the E- and H-planes, ease of fabrication, mechanical robustness, high gain, and cost-effectiveness [19].

The radiation behavior of TSAs is typically linearly polarized in the principal planes (E-plane and H-plane). However, elliptical polarization can occur between these two planes. Importantly, both the E-plane and H-plane exhibit nearly identical beamwidths while maintaining a low cross-polarization level, making the TSA a highly efficient antenna for millimeter-wave imaging systems [20].

3.4.Feeding Techniques

A feed line used in order to excite to radiate by direct contact. There are many different methods of feeding and four most popular methods:

- Microstrip Feed lines
- Aperture coupling feed
- proximity coupling
- Coaxial probe

- **Microstrip Feeding Lines**

A microstrip feed line is a conductive strip used to excite the radiating patch of an antenna. It is widely favored for its simple fabrication, straightforward design, and ease of achieving impedance matching, typically by adjusting the inset of the patch. The width of the feed line is generally narrower than that of the patch itself.

The main advantage of this feeding method is its simplicity. However, as the substrate thickness increases, surface wave excitation and feed line radiation also grow, which can limit the antenna's bandwidth. Proper impedance matching is achieved through the inset cut, aligning the feed line impedance with that of the patch, thereby eliminating the need for additional matching networks. Despite its convenience and modeling accuracy, the microstrip feed method experiences performance constraints due to increased spurious radiation and surface wave effects on thicker substrates, which reduces the effective bandwidth.

- **Aperture-Coupled Feeding**

In this method, a ground plane separates the feed line from the radiating patch, with energy transferred via a slot or aperture etched into the ground plane. The aperture is typically centered under the patch, which reduces cross-polarization effects.

The electromagnetic coupling strength depends on the aperture's size, shape, and placement. Isolation between the patch and feed line minimizes unwanted radiation. Designers often employ a high-permittivity lower substrate for the feed line and a thicker, low-permittivity upper substrate for the patch to optimize radiation efficiency. While this technique improves performance, it requires precise multi-layer alignment, making fabrication more complex.

- **Proximity Coupling**

Also known as electromagnetic coupling, this approach uses two dielectric layers. The microstrip feed line is embedded between the substrates, while the radiating patch sits on the top layer.

This method reduces spurious feed radiation and can achieve larger bandwidths—sometimes up to 13%—due to the increased overall antenna thickness. It also allows the use of different dielectric materials for the feed and patch layers, enabling optimization of individual layers. Impedance matching is accomplished by adjusting the feed line length and the patch-to-feed width ratio. However, the dual-layer configuration increases fabrication difficulty and antenna thickness, which can be a drawback in low-profile or highly compact applications.

- **Coaxial (Probe) Feeding**

The coaxial or probe feed technique involves inserting the inner conductor of a coaxial cable through the substrate and soldering it to the patch, while the outer conductor connects to the ground plane.

This method allows flexible placement of the feed point for precise impedance matching and produces minimal spurious radiation. It is relatively straightforward to implement. Nevertheless, coaxial feeding typically results in narrow bandwidth and requires drilling through the substrate, complicating analytical modeling. Additionally, for thicker substrates, the extended probe can introduce inductive effects that complicate impedance matching and affect planarity.

3.5. Antenna Performance Parameters

3.5.1. S-Parameters

S-parameters, or scattering parameters, quantify the power behavior of multi-port electrical networks. For antennas, S11 (reflection coefficient) is particularly important as it indicates the proportion of power reflected back from the antenna input relative to the incident power. Lower S11 values correspond to better impedance matching and more efficient radiation. Typically, an S11 value of -10 dB or lower is considered acceptable.

Mathematically, S11 in decibels is expressed as:

$$S_{11}(dB) = 10log\frac{V_-}{V_+} \qquad (3.1)$$

Where V_- is Reflected voltage, V_+ is Incident voltage

3.5.2. Radiation Patterns

A radiation pattern shows how the radiated power varies with direction from the antenna. This pattern is usually represented in polar or Cartesian coordinates and provides insight into the antenna's directivity and coverage. For millimeter-wave antennas, accurate characterization of the radiation pattern is essential to ensure focused energy delivery, which is critical in applications such as concealed image detection.

3.5.3. Directivity

Directivity is a fundamental characteristic of an antenna that quantifies its ability to focus radiated energy in a specific direction relative to an ideal isotropic radiator. An antenna that radiates energy equally in all directions is considered omnidirectional (or isotropic), possessing a directivity value of unity, which is equivalent to 0 dB [28].

For Circular microstrip antennas, the directivity can be expressed mathematically as:

$$D = \frac{1}{4\pi \int_0^{2\pi} 1 \int_0^{\pi} |F(\theta, \emptyset)|^2 sin\theta d\theta d\emptyset} \tag{3.2}$$

The equation tells as peak value of radiated power divided by average.

3.5.4. Gain

The **Gain** (G) of an antenna describes the ratio of the power density radiated in the direction of peak radiation to that of an ideal isotropic source. For instance, an antenna with a gain of **3 dB** indicates that the power received at a distance in the peak direction will be 3 dB higher (exactly twice as much) than the power received from a lossless isotropic antenna supplied with the same input power. [29].

$$G = \eta D \tag{3.3}$$

Whereηstands for antenna efficiency.

3.5.5. Antenna Efficiency

The efficiency of an antenna relates the power delivered to the antenna to the power radiated or dissipated within the antenna structure. A high-efficiency antenna radiates most of the power present at its input, whereas a low-efficiency antenna absorbs most of the power as internal losses or reflects it due to impedance mismatch. [30].

The losses associated within an antenna are typically the conduction losses (due to finite conductivity of the antenna) and dielectric losses (due to conduction within a dielectric, which may be present within an antenna). The antenna efficiency (or radiation efficiency) written as the ratio of the radiated power to the input power of the antenna and given by;

$$\eta = \frac{P_{rad}}{P_{in}} \tag{3.4}$$

Where P_{rad} radiated power, P_{in} is input power.

3.5.6. Bandwidth

Bandwidth is a fundamental antenna parameter that describes the range of frequencies over which the antenna can properly radiate or receive energy while maintaining acceptable performance characteristics, such as gain, radiation pattern, and impedance matching.

The desired bandwidth is often a primary constraint in antenna selection. For instance, many antenna types, such as standard microstrip patches, are inherently narrowband and cannot be used for wideband operations without specific optimization [31].

3.5.7. Polarizations

An antenna is a transducer that converts radio frequency electric current to electromagnetic waves that radiate into space. The electric field plane determines the polarization or orientation of the radio wave. In general, most antennas radiate in either a linear or a circular polarized manner. A linearly polarized antenna radiates wholly in one plane containing the direction of propagation, whereas in a circularly polarized antenna, the plane of polarization rotates in a circle, making one complete revolution during one period of the wave. If the rotation is clockwise looking in the direction of propagation, the sense **is** called Right-Hand Circular (RHC). If the rotation is counter-clockwise, then it **is** called Left-Hand Circular (LHC) [32].

3.5.8. Return Loss

Return loss is an important parameter when testing an antenna. It **is** related to impedance matching and the maximum power transfer theory. It is also a measure of the effectiveness of an antenna to deliver power from the source to the antenna. The return loss (RL) **is** defined by the ratio of the incident power of the antenna to the power reflected back from the antenna to the source [33].

$$RL = 10log_{10}\frac{P_{in}}{P_{ref}}\ in\ dB \tag{3.5}$$

Where RL is return loss, P_{in} is incident power, P_{ref} is reflected power.

3.5.9. Voltage Standing Wave Ratio (VSWR)

There should be a maximum power transfer between the transmitter and the antenna for the antenna to perform efficiently. This happens only when the input impedance Zin matched to the transmitter impedance, Zs [34].

In the process of achieving this particular configuration, any impedance mismatch results in a reflection of power, which leads to the formation of standing waves. This characteristic is quantified by the Voltage Standing Wave Ratio (VSWR), which is given by:

$$VSWR = \frac{V_{max}}{V_{min}} = \frac{1 + \Gamma}{1 - \Gamma} \qquad (3.6)$$

Where V_{max} is maximum voltage, V_{min} is minimum voltage, Γ is reflection coefficients

3.5.10. Why and What 24GHz

The 24 GHz technology has been well known since 2001, when the Federal Communications Commission (FCC) established the unlicensed band range. Note that for many years, millimeter-wave (mm-wave) technology was primarily deployed for military applications. The opening of a license-free 7 GHz band (from 57 to 64 GHz) and the 24 GHz ISM band—which stands for “Industrial, Scientific, and Medical”—has created opportunities and challenges for researchers to utilize these frequencies.

The 24 GHz band offers a much shorter wavelength, resulting in more stable and predictable signal propagation. This significantly boosts imaging performance, enabling the system to identify, locate, and image various objects with high precision. Furthermore, the short wavelength makes propagation more stable; with minimal multipath effects, signal strength remains consistent over time and is strongly correlated with propagation distance. This increases the robustness of the imaging design [35].

3.5.11. Properties of 24GHz for Imaging [36].

- 24GHz characterized by non-ionized radiation.
- The wave can penetrate clothing and reflected from concealed object are used in millimeter wave scanners for airport security scanning.
- The wave transmitted or reflected from the target cannot identify the specific material rather expose the shape, size and position of concealed objects.

- 24GHz cannot interrupted by bad atmosphere, snow, fog, dust than microwave.
- 24GHz characterized by optical propagation which can be reflected by small metal surface and focused by dielectric lens of diameter from 5 to 30cm, because the wavelength much smaller than the equipment that manipulates them.
- Dielectric and other organic materials are transparent to millimeter wave such applications are scanners to detect weapon and other dangerous material under dielectric material used for airport security.

Table 3.1. Electrical Properties of human body tissue parameters at 24GHz described below table [37].

Tissue	Relative permittivity	Loss tangent
Dry skin	7.98	1.37
Wet skin	10.2	1.16
Muscle	12.9	1.23

Based on the data, human muscle tissue has a higher dielectric constant and conductivity than skin, allowing it to interact more with electromagnetic energy. This means that objects concealed behind human muscle are generally more detectable than those behind wet skin, followed by dry skin and fat, respectively, at the 24 GHz millimeter-wave band. Conversely, objects concealed within fat are less detectable than those in other tissues at these frequencies due to the lower water content and different dielectric properties of adipose tissue

3.5.12. 24GHz Antenna

There is a wide variety of millimeter-wave antennas, including Yagi-Uda, hybrid, stacked, bow-tie, circular patch, and tapered slot antennas. Among these, antennas with end-fire radiation characteristics are generally preferred for millimeter-wave imaging over broadside antennas, as they provide higher gain and greater sensitivity for target detection.

Consequently, for the design of a millimeter-wave (MMW) imaging scanner, Tapered Slot Antennas (TSAs) are considered an optimum choice. They offer end-fire radiation characteristics, a low profile, high efficiency, and symmetric radiation patterns in both the E and H planes. Additionally, they are easy to fabricate, durable, high-gain, and cost-effective [38].

While the radiation pattern is linearly polarized in the primary planes, elliptical polarization may exist between the E and H planes. Notably, the E and H planes exhibit almost identical beamwidths, and the cross-polarization levels remain low.

3.6. Circular Patch Antenna

A circular patch antenna is a compact, low-profile radiating element that can be easily integrated onto planar surfaces. It comprises a thin metallic patch with a circular geometry, positioned above a larger conductive ground plane and separated by a dielectric substrate. This combination forms a resonant cavity, where the resonance is primarily dictated by the patch radius. For a circular patch, the fundamental resonant mode (TM_{110}) occurs when the radius is roughly proportional to the operating wavelength.

Radiation occurs mainly due to fringing fields at the edges of the patch, which make the antenna's effective electrical size slightly larger than its physical dimensions. To account for this effect, the actual radius is designed to be marginally smaller than the ideal theoretical radius needed for resonance.

Circular patch antennas are especially well-suited for millimeter-wave frequencies because the short wavelengths allow for highly compact designs. Their straightforward fabrication on printed circuit boards (PCBs) makes them ideal for portable communication and imaging devices. Moreover, arranging multiple patches on a single substrate enables the creation of microstrip arrays, which can provide high gain and support phased-array configurations with electronically steerable beams, enhancing system performance for advanced applications.

3.6.1. Requirements of 24GHz Circular Patch antenna for Imaging [40].

- Dielectric Lens
- Wide band width
- Millimeter wave frequency
- Narrow beam width
- High total gain
- High total directive gain
- Low reflection coefficient
- Low voltage standing wave ratio
- Low side lobe level

3.6.2. Dielectric Lens

24 GHz propagation basically requires a high-gain antenna and high efficiency. A dielectric lens focuses radiated energy to increase the gain of the antenna [41].

A spherical lens antenna is suitable for imaging and sensing systems that need to enhance the directive beam of the antenna. The spherical lens is homogeneous and suitable for most antenna designs because of its simple structure and ease of integration. It also has the ability to collect beams from multiple directions. The type of substrate, the diameter, and the distance between the lens and the antenna play an important role in increasing the gain of the antenna.

3.6.3. Imaging System Performance

The device used to measure the performance of active mono-static imaging system is resolutions, Distance, Pixel and Field of Views which summarized below.

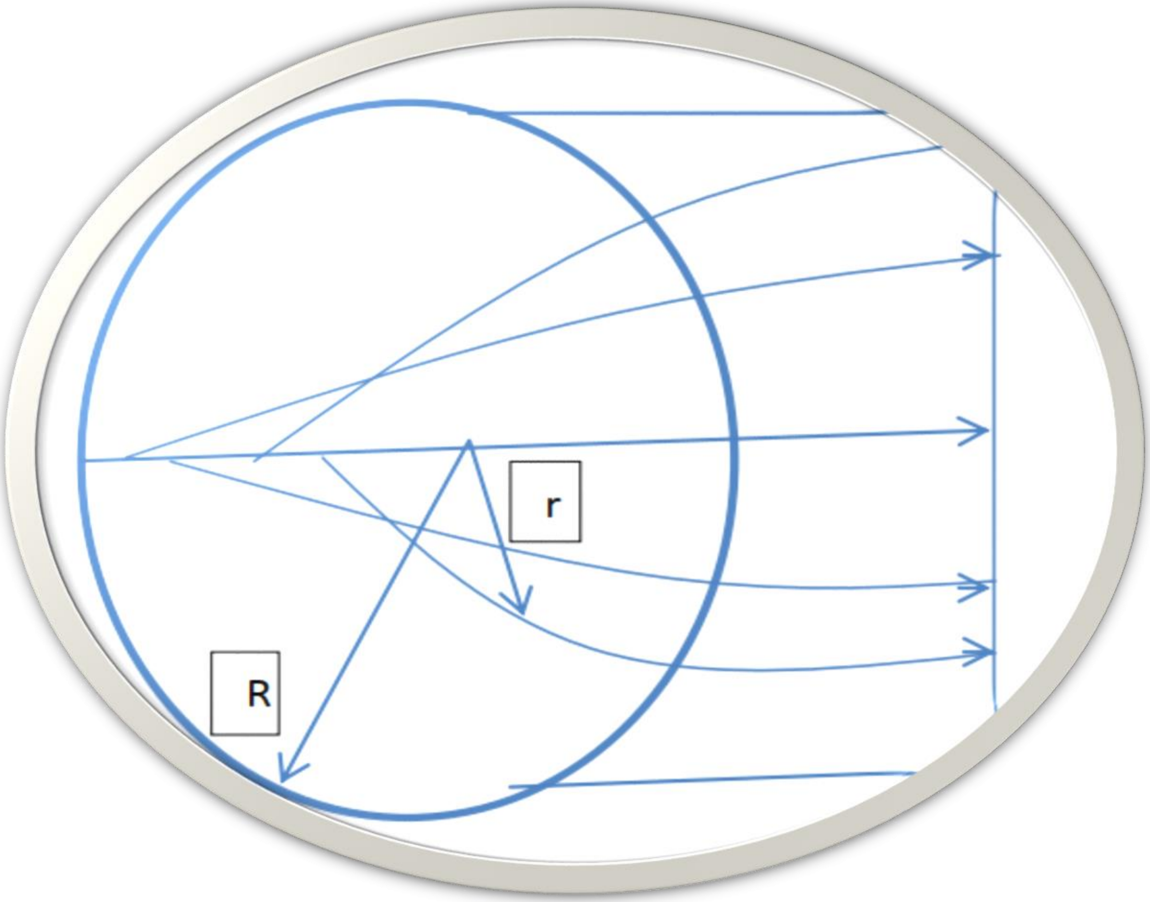

Figure 2 Dielectric Lens

Relative permittivity and radius of lens related by;

$$\varepsilon_r = 2 - (\frac{r}{R})^2 \quad (3.7)$$

Where R radius and r refractive index given by:

$$n(r) = N(R)[2 - (r/R)^2]^{1/2} \quad (3.8)$$

3.6.4. Spatial Resolution

Spatial resolution is a point pixel size of image object described in terms of pixel per line, dot per inch or lines per millimeter. The resolution of antenna detects the picture which depends on the main beam of narrower beam that guides to large antenna [42].

The spatial resolution of an imaging system is known as field of views. The distance from antenna to target determined based on spatial resolution of an image.

3.6.5. Method of Analysis

Circular patch antenna is type of microstrip antenna which consists of thin circular metal patch, dielectric substrate, ground plane. Assume Circular patch made from thin copper and used to radiate electromagnetic waves. A Dielectric substrate Insert in between patch and ground plane used as insulating material that separate radiating patch and ground plane. Ground plane used as a ground for designed antenna. The dimensions of those parameters analyzed by modified wolf model.

3.6.6. Modified Wolf Model

Modified wolf model considers circular patch antenna as equivalent of Circular patch antenna as shown in figure below.

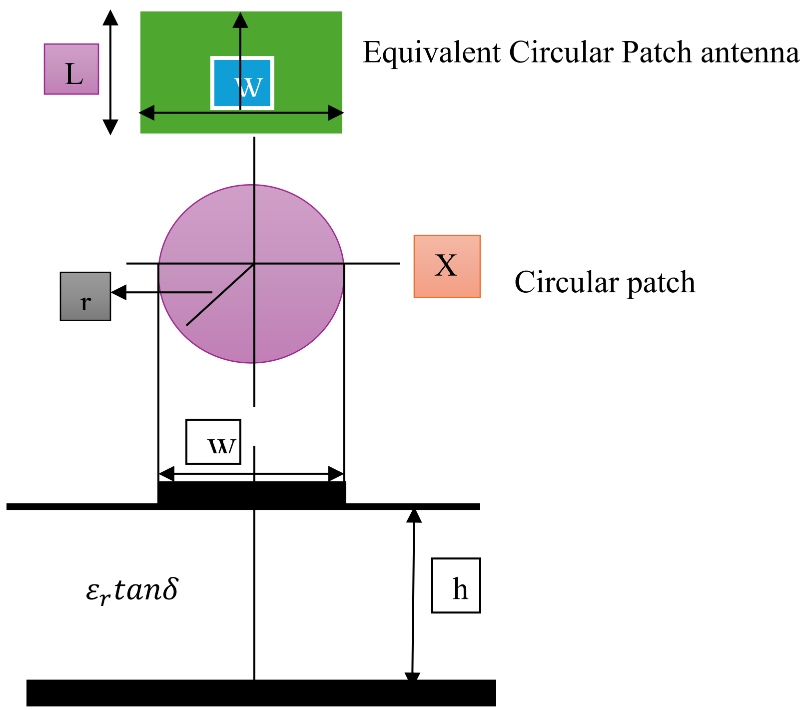

Figure 3 Circular patch antenna and equivalent Circular patch antenna on thin substrate

The width of equivalent Circular patch antenna is equal to equivalent diameter of circular patch antenna. The diameter giving the width of the equivalent Circular. This choice of width includes the maximum dimension of the circular patch in the equivalent Circular patch and given by;

$$W = 2r \tag{3.9}$$

where w is width of Circular patch antenna which equivalent to diameter of circular patch antenna, r is radius of circular patch antenna and given by;

$$r = \frac{F}{\{1 + \frac{2h}{\pi \varepsilon F} \ln \left[(\frac{\pi F}{2h}) + 1.7726 \right] \}^{1/2}} \tag{3.10}$$

where $F = \frac{8.791 \times 10^9}{f_r \sqrt{\varepsilon}}$, h is height, ε is permittivity of dielectric substrate.

The length of circular patch antenna equivalent to Circular is obtained by using the invariance of the electrostatic energy below both the Circular and circular patches and given by;

$$L = \frac{\pi r}{2} \tag{3.11}$$

The fringe capacitance computed along two sides of the equivalent Circular patch is assumed identical to the fringe capacitance of the circular patch [43].

The Patch is inside the circular patch, therefore there is no fringe fields along the width sides. However, when transforming a circular patch of smaller diameter to the equivalent Circular patch, bend occurs in the fringing electric fields. This is accounted for by adding values for the two-corner capacitance of the equivalent Circular patch [44].

The total lumped capacitance of equivalent Circular patch is given by;

$$C_t = C_o + 2C_e + C_c \tag{3.12}$$

Where C_t is total Capacitance, C_o is central capacitance, C_e fringe capacitance and C_c is corner capacitance. Central capacitance of equivalent Circular patch antenna is given by;

$$C_o = \frac{\varepsilon_r \varepsilon_0 \pi r^2}{h} \tag{3.13}$$

where ε_r is relative permittivity, ε_0 permittivity in free space, r is radius and h are height of dielectric substrate. Fringing capacitance of equivalent Circular patch given by;

$$C_e = \frac{1}{2}\left[\left(\frac{Z_0 L}{V_0 Z^2}\right) - C_o\right] \tag{3.14}$$

Where V_0 is speed of light, Z_0 is characteristics impedance of microstrip line, Z is frequency dependent characteristic impedance and given by;

$$Z = \frac{Z_0}{\sqrt{\varepsilon_{r(f)}}} \tag{3.15}$$

The width of feed lines depends on characteristics impedance of antenna [45].

Characteristics impedance of antenna depend on height and width of equivalent Circular patch antenna and given by;

$$Z_0 = \frac{24.411}{\sqrt{\varepsilon_{eff}}} ln \frac{8h}{W_0} + \frac{W_0}{4h} \ , when \ \frac{W_0}{h} < 1 \tag{3.16}$$

Where effective dielectric constant, this height, W_0 is width, characteristic impedance of equivalent microstrip circular patch antenna different for ratio of width to height is greater than one and given by;

$$Z_0 = \frac{120\pi}{\sqrt{\varepsilon_{eff}}[\frac{W_0}{h} + 1.393 + 0.667\ln(\frac{W_0}{h} + 1.4444)]}, \frac{W_0}{h} > 1 \tag{3.17}$$

Where ε_{eff} is effective dielectric constant given by;

$$\varepsilon_{eff} = \frac{\varepsilon_r + 1}{2} + \frac{\varepsilon_r - 1}{2\sqrt{1 + \frac{12h}{W_0}}} \tag{3.18}$$

Due to fringing field at equivalent length of Circular patch microstrip patch antenna effective length of antenna is different from actual length of antenna and given by;

$$L_{eff} = L + 2\Delta L_{eff} \tag{3.19}$$

where L_{eff} is effective length of antenna, The effective length therefore is differing from the physical length by ΔL_{eff}, the ratio of $\Delta 2L_{eff}$ to h is given by;

$$\frac{\Delta 2L_{eff}}{h} = 0.412\frac{(\varepsilon_{reff} + 0.3)(\frac{W_0}{h} + 0.264)}{(\varepsilon_{reff} + 0.258)(\frac{W_0}{h} + 0.8)} \tag{3.20}$$

Resonant frequency of circular microstrip antenna is the function of effective dielectric constants and given by;

$$fr = \frac{V_0}{2\sqrt{\varepsilon_{reff}}(L + 2\Delta L_{eff})} \tag{3.21}$$

Where V_0 is speed of light, L is physical length, L_{eff} is length extension due to fringing fields, The feed location of single circular patch antenna is one third distance from center of patch [46]

and given by;

$$y_f = \frac{W}{2} \tag{3.22}$$

Where y_f is locations of feed line to y directions, and location of feed lines to the x directions is given by;

$$x_f = \frac{L}{\sqrt{\varepsilon_{r,\ eff,\ L}}} \tag{3.23}$$

Where x_f is locations of feed lines to x directions.

CHAPTER FOUR

DESIGN

4.1. Introductions to Antenna Design

This design describes a compact aperture-coupled circular microstrip antenna optimized for millimeter-wave (mm Wave) operation at 24GHz. A dielectric plano-convex lens is added to enhance gain and directivity for 5G and imaging applications. All parameters are ready for HFSS simulation setup.

4.2.Design Considerations

The dual-layer design employs separate substrates for the radiating element and the feed structure. By using a slot-coupled feeding mechanism, surface wave excitation is minimized, and impedance matching is enhanced. Additionally, integrating a dielectric lens directs and concentrates the radiated energy, resulting in increased gain at 24 GHz.

Table 4.1. Design Considerations

Parameter	**Symbol**	**Value**	**Description**
Operating frequency	f_0	24GHz	Target mm Wave band
Wavelength	$\lambda_0 = \frac{c}{f_0}$	5mm	Free-space wavelength
Upper substrate	ε_{r1}, h_1	2.2, 0.254 mm (Rogers RT5880)	Radiating layer

Lower substrate	ε_{r2}, h_2	2.94, 0.508 mm (Rogers 4003C)	Feed layer
Feed technique	–	Aperture-coupled	Ensures isolation and low spurious radiation
Lens material	ε_L	2.1 (Teflon /PTFE)	Low-loss dielectric

4.3.Design the Circular Patch

4.3.1. Design Procedures

Step 1: Calculate the Circular Patch Radius

The patch radius determines the resonant frequency. Slight changes in (a) shift the frequency, so precision is essential at mm Wave frequencies.

For the dominant TM_{11} mode, the patch radius (a) is obtained using:

$$a = \frac{F}{\sqrt{1 + \frac{2h_1}{\pi \varepsilon_{r1} F}\left[\ln\left(\frac{\pi F}{2h_1}\right) + 1.7726\right]}}$$

Where:

$$\mathrm{F} = \frac{8.791 \times 10^9}{\mathrm{f}_0 \sqrt{\varepsilon_{\mathrm{r1}}}}$$

$$\mathrm{F} = \frac{8.791 \times 10^9}{24.411 \times 10^9 \sqrt{2.2}}$$

$$\mathrm{F} = 0.0420$$

The Radius will be:

$$a = \frac{F}{\sqrt{1 + \frac{2h_1}{\pi \varepsilon_{r1} F} \left[\ln\left(\frac{\pi F}{2h_1}\right) + 1.7726 \right]}}$$

1. Compute the logarithmic term:

$$\frac{\pi F}{2h_1} = \frac{3.14 \times 0.0420}{2 \times 0.000254} = 259.4$$

$$\ln(259.4) = 5.56$$

Add constant

$$5.56 \; + \; 1.7726 \; = \; 7.33$$

2. Compute multiplier term:

$$\frac{2h_1}{\pi \varepsilon_{r1} F} = \frac{0.000508}{0.290} = 0.00175$$

$$1 + \frac{2h_1}{\pi \varepsilon_{r1} F} = 1 + 0.00175(7.33) = 1.0128$$

$$\sqrt{1.0128} = 1.006$$

3. Substitute back:

$$a = \frac{0.0420}{1.006} = 4.18mm$$

Patch radius a = 4.18 mm

Step 2: Determine Patch diameter

$$\mathrm{P_d} = \mathrm{a} \times 2$$

$$\mathrm{P_d} = 4.18mm \times 2$$

$$\mathrm{P_d} = 8.36mm$$

Step 3: Verify the Resonant Frequency

Effective patch radius is adjusted as:

$$a_{eff} = a\sqrt{1 + \frac{2h_1}{\pi a \varepsilon_{r1}}\left[\ln\left(\frac{\pi a}{2h_1}\right) + 1.7726\right]}$$

Compute:

$$\frac{\pi a}{2h_1} = \frac{3.1416(0.004175)}{2(0.000254)} = 25.8$$

$$\ln(25.8) = 3.25$$

$$3.25 + 1.7726 = 5.02$$

$$\frac{2h_1}{\pi \varepsilon_{r1} F} = \frac{0.000508}{0.0288} = 0.0176$$

$$1 + \frac{2h_1}{\pi \varepsilon_{r1} a} = 1 + 0.0176(5.02) = 1.088$$

$$\sqrt{1.088} = 1.043$$

1. Substitute back:

$$\mathrm{a_{eff}} = 0.004175 \times 1.043 = 0.00435\mathrm{m}$$

Now, the resonant frequency is:

$$f_r = \frac{1.8412c}{2\pi a_{eff}\sqrt{\varepsilon_{r1}}}$$

$$f_r = \frac{1.8412 \times 3 \times 10^8}{2 \times 3.14 \times (0.00435)\sqrt{2.2}}$$

$$\mathrm{f_r} = 24.411\mathrm{GHz}$$

Resonant frequency ≈ 24.411GHz, which aligns perfectly with the 24GHz target.

This validation ensures that the chosen dimensions will produce resonance near the target frequency before full simulation.

Step 4: Ground Plane and Feed Slot Design

The slot acts as a magnetic dipole coupling energy from the feed line to the upper patch. Adjusting slot size affects bandwidth and impedance matching.

A slot is cut on the ground plane for aperture coupling.

Table 1.2 Ground Plane and Feed Slot Design

Parameter	**Symbol**	**Typical Value**	**Remarks**
Slot length	L_s	≈ λ_g/ 2 = 2 mm	$\lambda_g \approx \lambda_0 / \sqrt{\varepsilon r_2}$
Slot width	W_s	0.3 – 0.5 mm	Start with 0.4 mm
Feed impedance	Z_0	50 Ω	Determined below

Step 5: Determine Feedline Width (50 Ω)

For a microstrip line on the lower substrate:

$$Z_0 = \frac{24.411}{\sqrt{\varepsilon_{eff}}} \ln \left(\frac{8h_2}{W_f} + \frac{W_f}{4h_2}\right.$$

The effective dielectric constant is approximated as:

$$\varepsilon_{\mathrm{eff}} = \frac{\varepsilon_{\mathrm{r2}} + 1}{2} + \frac{\varepsilon_{\mathrm{r2}} - 1}{2}\left(1 + \frac{12\mathrm{h}_2}{\mathrm{W_f}}\right)^{-0.5}$$

Iteration:

- $\mathrm{W_f} = 1.0\mathrm{mm} \Rightarrow \mathrm{Z_0} \approx 105\Omega$ (too high
- $\mathrm{W_f} = 1.5\mathrm{mm} \Rightarrow \mathrm{Z_0} \approx 70\Omega$
- $\mathrm{W_f} = 2.0\mathrm{mm} \Rightarrow \mathrm{Z_0} \approx 52\Omega$

Feedline width (W_f = 2.0 mm) provides ≈ 50Ω.

Feedline length (L_f = 5mm) (fine-tuned in HFSS).

The feedline is optimized for impedance matching. A 50 Ω line ensures minimal reflection at the feed port.

4.4.Lens Design

(a) Material

Teflon (PTFE): (ε_L = 2.1)

Step 1: Determine Linear refractive index of a material

$$n_L = \sqrt{\varepsilon_L}$$

$$n_L = \sqrt{2.1}$$

$$n_L = 1.45$$

(b) Focal Geometry

Step 2: Determine Focal Geometry

For a plano-convex lens:

$$f = \frac{R}{n_L - 1}$$

Using (R = 7.5 mm):

$$f = \frac{7.5mm}{1.45 - 1}$$

$$f = 16.7 \text{ mm}$$

(c) Lens Size

Step 3: Determine Lens Size

$$\mathrm{D_L} = 3\lambda_0$$

$$\mathrm{D_L} = 3(5 \text{ mm})$$

$$\mathrm{D_L} = 15 \text{ mm}$$

Table 4.3 Summary of Lens dimensions:

Parameter	Symbol	Value
Radius of curvature	R	7.5 mm
Focal length	F	16.7 mm
Lens diameter	D_L	15 mm
Thickness (center)	T	3-4 mm

The dielectric lens focuses the beam and improves directivity. Its distance from the patch (≈ focal length) gives the highest gain.

4.5.HFSS Simulation Setup

Table 4.4 Geometry (in mm)

Part	Description	Key Parameters
Patch	Circular copper	Radius = 4.18
Upper substrate	Rogers RT5880	ε_{r1} = 2.2, h_1 = 0.254
Ground	PEC plane with slot	Slot L = 2.0, W = 0.4
Lower substrate	Rogers 4003C	ε_{r2} = 2.94, h_2 = 0.508
Feedline	Microstrip line	W = 2.0, L = 5.0
Lens	Teflon plano-convex	D = 15, R = 7.5, f = 16.7, t = 3.5

Air box	Radiation boundary	Clearance ≥ $\lambda_o/4$ (≈ 1.25 mm)

4.5.1. Boundary and Excitation

- Apply radiation boundary to the air box.
- Use wave port at feedline input.
- Assign finite copper conductivity if desired.

4.5.2. Frequency Sweep

- Range: 1–50 GHz
- Step: 0.1 GHz

4.5.3. Meshing

- Minimum mesh ≈ λ_o / 20 = 0.25 mm.
- Refine mesh near slot and lens edges for accuracy.

CHAPTER FIVE

SIMULATION RESULTS, DISCUSSIONS AND ANALYSIS

5.1.Result and Discussions

This chapter presents results and discussions of single circular patch antenna with and without Lens, Double layer circular patch antenna with Lens and without Lens, for MillimeterWave Concealed Image Detections systems.

5.2.Simulation Results of single circular patch antenna

The Below designs are single circular patch antenna without lens in High frequency simulations software.

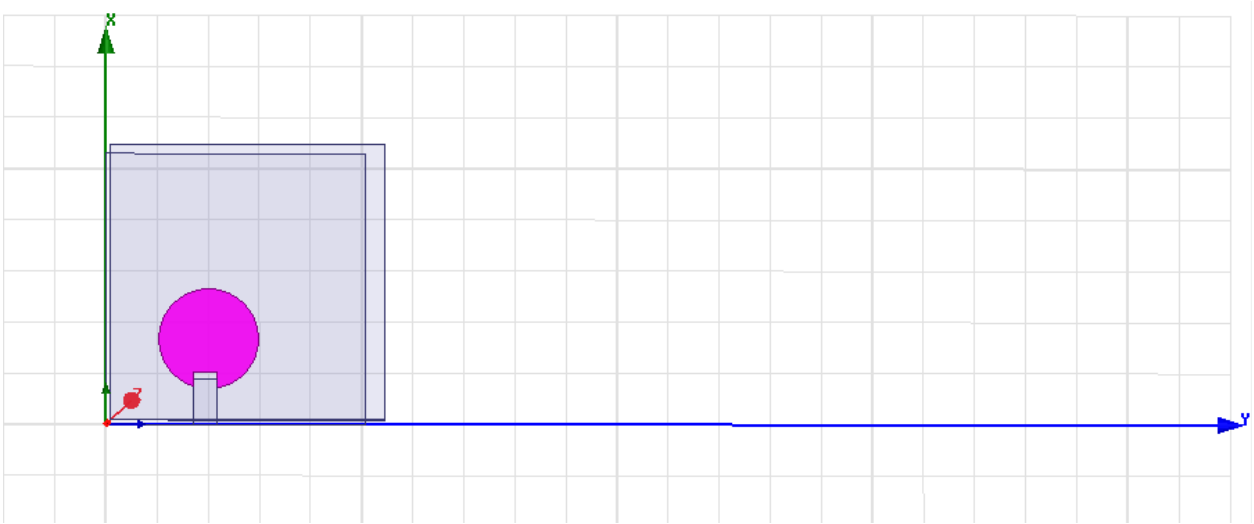

Figure 4 single circular patch antenna

5.2.1. Gain of Single Circular Patch Antenna

Simulation results from HFSS indicate that the single circular patch antenna, operating at 24.411 GHz, achieves a gain of approximately 9.76dB. While adequate for basic millimeter-wave imaging tasks, this level of gain is limited for high-resolution or long-range applications. At this frequency, antenna gain is a key factor influencing image clarity, spatial resolution, and the effective detection distance.

The moderate gain provided by this configuration allows for acceptable short-range imaging performance, but the broader beamwidth restricts energy concentration, resulting in lower image sharpness and reduced detection range. In practical imaging scenarios, this limitation can reduce contrast and hinder the identification of fine features, especially at distances beyond the near-field region.

This analysis establishes a quantitative link between antenna gain and imaging performance at 24.411 GHz, serving as a baseline for further improvements. To meet the demands of advanced millimeter-wave image detection and concealed object sensing systems, strategies such as multi-element arrays, lens integration, or structural optimization are required to enhance radiation intensity and improve overall imaging resolution.

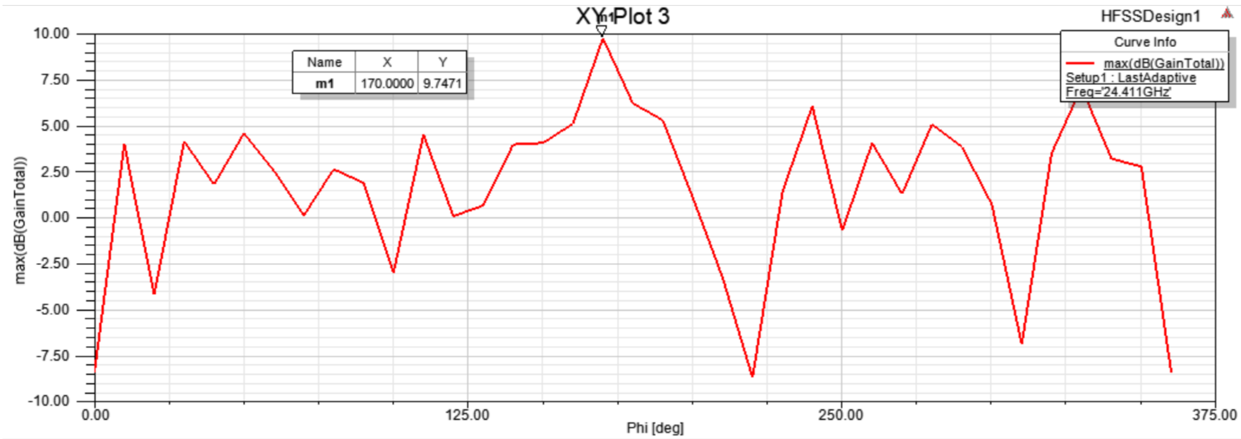

Figure 5 Total Gains of single CPA

5.2.2. Directivity of Single Circular Patch Antenna

HFSS simulations indicate that the single circular patch antenna operating at 24.411 GHz exhibits a directivity of approximately 10.09 dB. While this level is sufficient for fundamental millimeter-wave imaging tasks, it is limited for high-resolution applications. At this millimeter-wave frequency, antenna directivity plays a crucial role in shaping the radiated beam, influencing image sharpness, spatial resolution, and the effective detection distance.

The observed moderate directivity produces a relatively wide radiation pattern, which is adequate for short-range imaging but restricts energy concentration. As a result, image contrast and spatial resolution—typically around 6–7 mm—are constrained, limiting reliable detection to near-field distances of roughly 1–3 m.

This analysis establishes a clear relationship between antenna directivity at 24.411 GHz and practical imaging performance. It demonstrates that while a lens-free single circular patch antenna can serve compact, short-range imaging systems, higher directivity is essential in advanced millimeter-wave concealed image detection setups to improve radiation efficiency, extend detection range, and enhance image clarity.

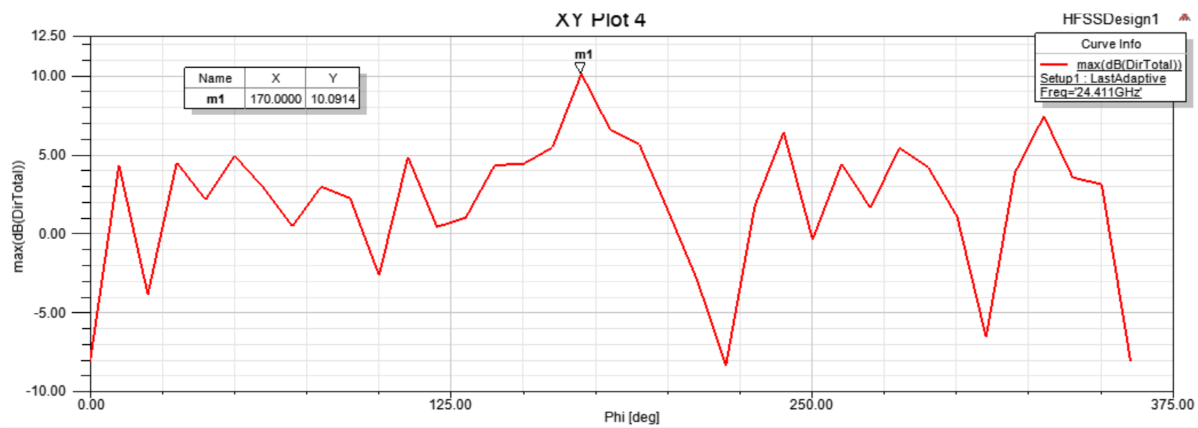

Figure 6 Total Directivity of single CPA

5.2.3. S11 of single circular patch antenna

HFSS simulation results reveal that the single circular patch antenna at 24.411 GHz achieves a reflection coefficient of approximately -17.34 dB, indicating excellent impedance matching and efficient power delivery to the radiating element. Such low reflection ensures that most of the input energy is radiated, enhancing the received signal strength, improving the signal-to-noise ratio, and stabilizing phase information, all of which are critical for high-fidelity millimeter-wave image reconstruction.

The simulated antenna bandwidth, measured between the -10 dB return loss points, spans over 42 GHz, providing a remarkably broad operational range around the 24.411 GHz center frequency. This extensive bandwidth supports superior imaging performance by allowing finer range resolution (on the order of millimeters), better target distinction, and minimized range ambiguity. It also ensures consistent image clarity for short-range detection distances of roughly 1-3 m.

This study highlights that combining precise impedance matching with an ultra-wide operational bandwidth significantly enhances millimeter-wave imaging performance, even with a single patch antenna. Such characteristics make the design particularly suitable for compact, high-speed, short-range imaging systems used in concealed object detection and other millimeter-wave sensing applications.

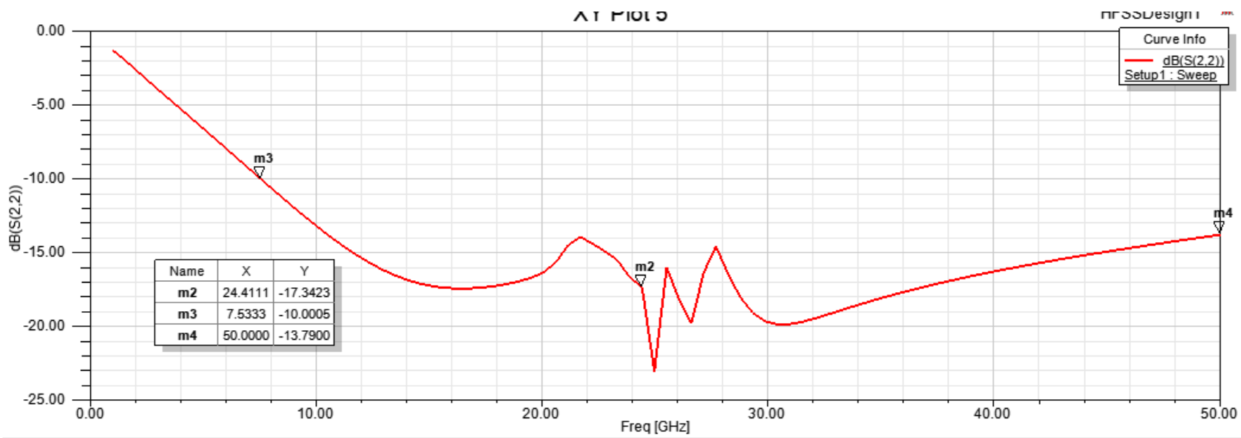

Figure 7 Reflection Coefficient of single CPA

5.2.4. Voltage Standing Wave Ratio of Single CPA

The HFSS simulations indicate that the single circular patch antenna operating at 24.411 GHz exhibits a Voltage Standing Wave Ratio (VSWR) of approximately 2.3, which falls comfortably below the common 3 dB threshold. This confirms that the impedance between the feed line and the radiating patch is well-matched, allowing over 75% of the input power to be effectively delivered to the antenna.

Such efficient power transfer directly contributes to higher radiation efficiency, improving the strength of received signals and stabilizing both amplitude and phase information key factors for reliable millimeter-wave image reconstruction. In practical imaging scenarios, this level of performance supports spatial resolution on the order of 6–7 mm and ensures consistent detection of objects within short-range distances of roughly 1-3 m.

This analysis demonstrates that maintaining a low VSWR at the optimal 24.411 GHz frequency is sufficient to support stable, broadband millimeter-wave image detection. Moreover, the findings suggest that further optimization of impedance matching and radiation efficiency could enhance detection range and improve overall image fidelity in high-performance concealed imaging systems.

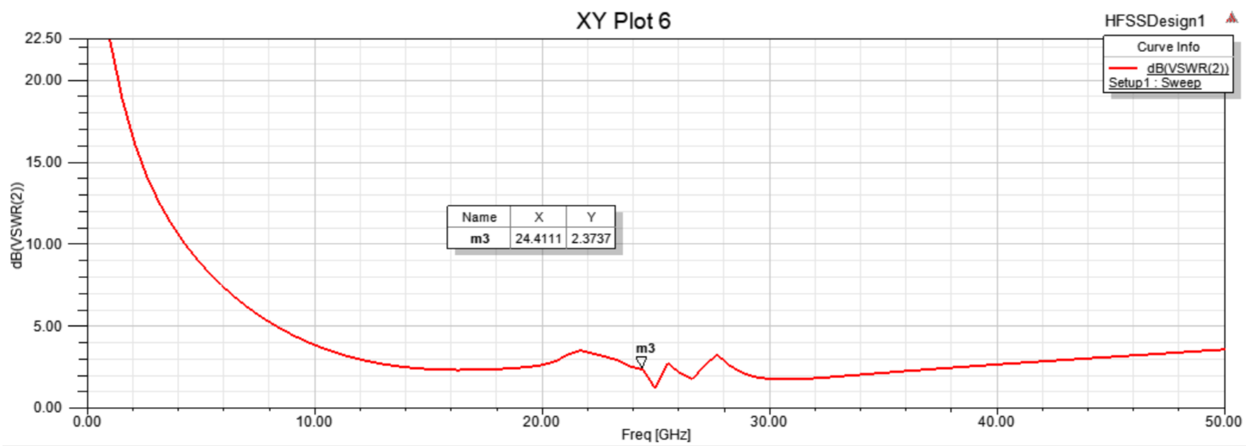

Figure 8 VSWR of single CPA

5.2.5. Radiation Patterns of Single CPA

The Radiation Patterns of Single circular patch antenna at 24.411Ghz for millimeters wave Concealed Image Detections has been looks like below diagrams.

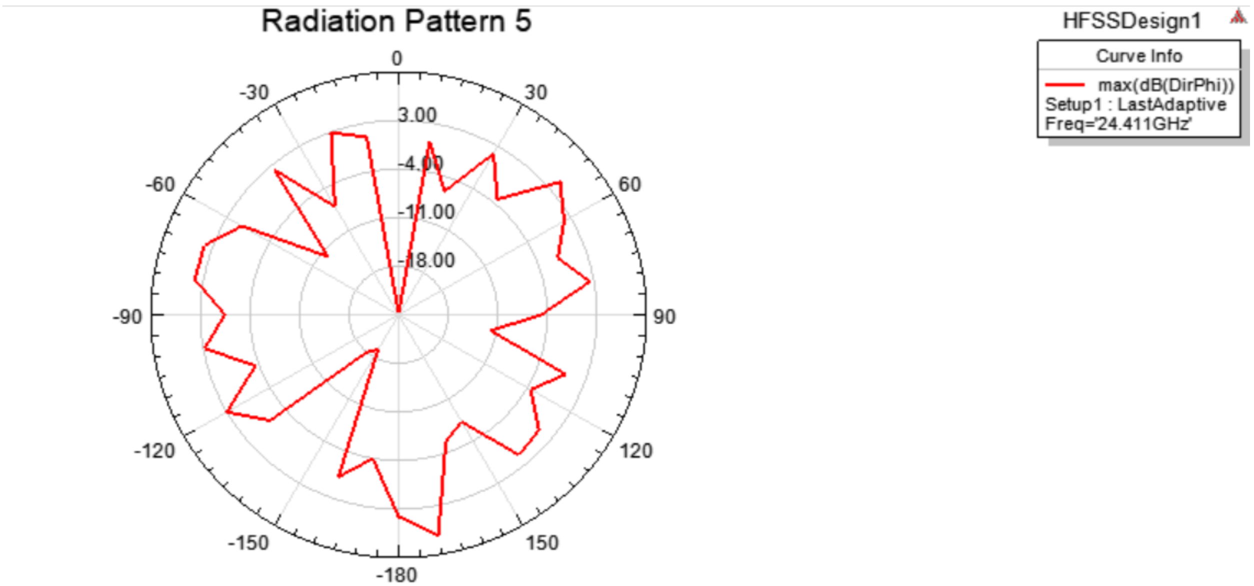

5.6. Radiation Patterns of Single CPA

5.2.6. 3D Polar Plot of Single CPA

The 3D polar plots of Single circular patch antenna at 24.411Ghz for millimeters wave Concealed Image Detections has been looks like below diagrams.

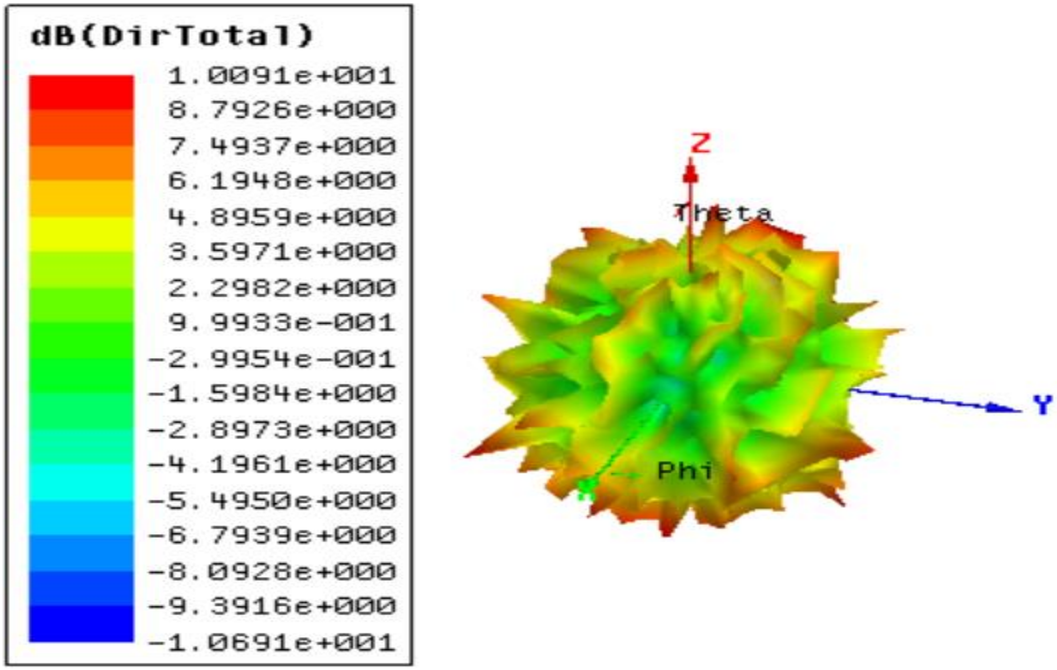

Figure 9 3D Polar plots of Single CPA

5.4.Simulation Results of double Layer Circular patch antenna without Lens

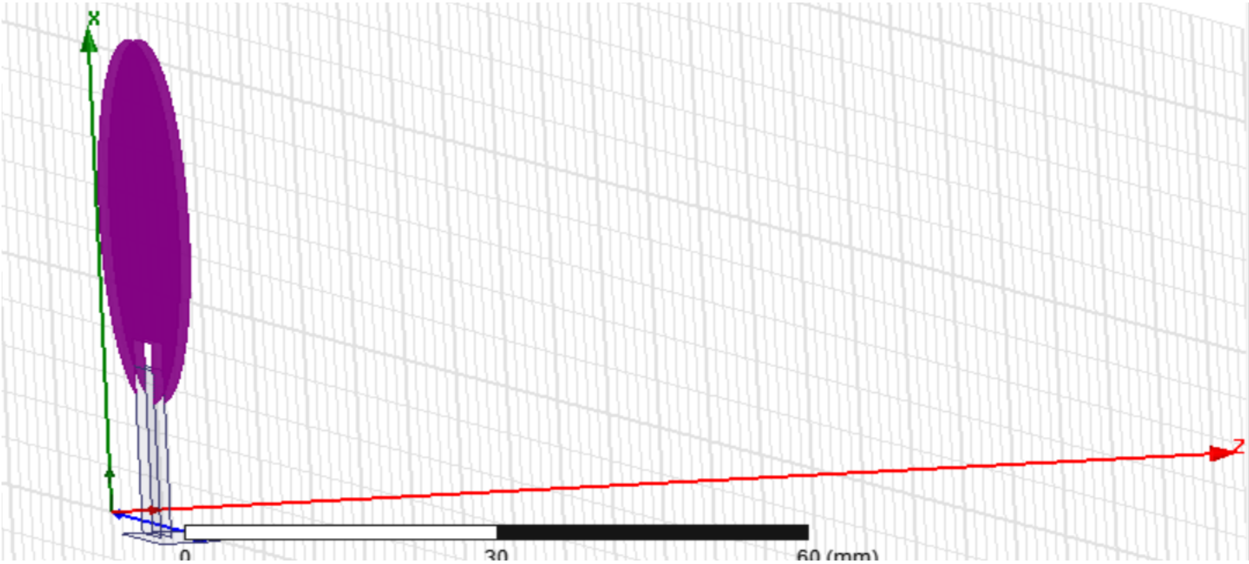

Figure 10 Simulation Results of double Layer Circular patch antenna without Lens

5.4.1. Gain of double Layer circular patch antenna

HFSS simulations indicate that the double-layer circular patch antenna operating at 24.411 GHz achieves a total gain of approximately 12.8dB. While this gain remains moderate for high-end millimeter-wave imaging applications, it marks a significant improvement over the single-layer design, offering nearly a 3 dB increase. This enhancement effectively doubles the radiated power, directly boosting imaging performance.

The higher gain improves signal-to-noise ratio, enabling sharper spatial resolution in the range of 5–6 mm and extending the practical detection range to about 2-5 m. At this optimal millimeter-wave frequency, the double-layer configuration demonstrates that layering the dielectric substrate can enhance radiation efficiency and overall imaging capability without adding undue complexity to the antenna structure.

These results establish a quantitative relationship between gain improvement and millimeter-wave imaging performance, providing a practical design approach for developing higher-resolution, longer-range concealed image detection systems that require stronger, more focused radiation patterns.

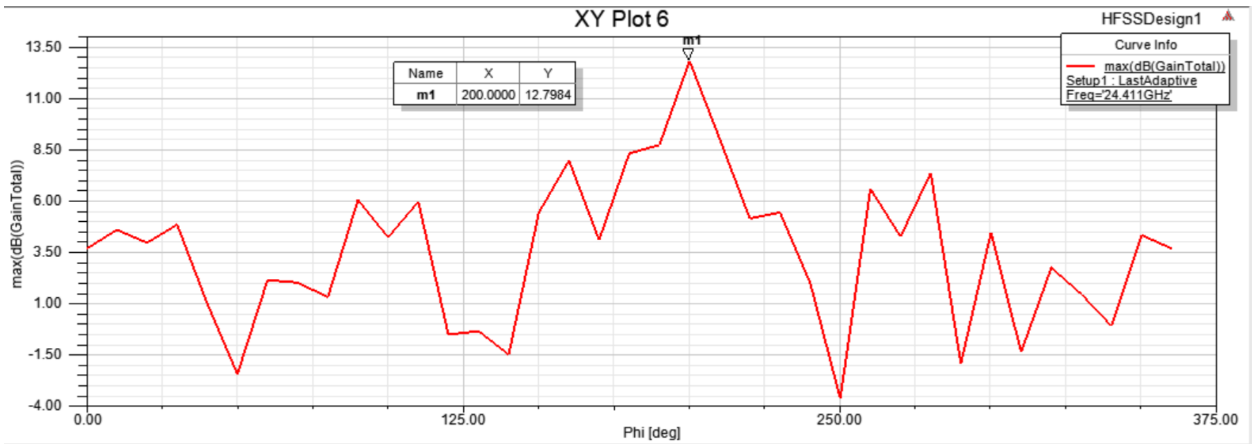

Figure 11 Total Gains of Double Layer CPA

5.4.2. Directivity of Double Layer circular patch antenna

HFSS simulations show that the double-layer circular patch antenna at 24.411 GHz achieves a total directivity of approximately 13.05dB. Although this value is moderate for advanced millimeter-wave imaging applications, it represents a clear improvement over the single-layer antenna, with roughly a 3 dB increase in beam concentration. This enhancement focuses the radiated energy more effectively within the imaging region, resulting in improved image contrast and clarity.

From a practical imaging standpoint, the increased directivity supports finer spatial resolution, reducing it to around 5–6 mm, and extends the effective detection range to roughly 2–5 m for short-range concealed object detection. At this optimal millimeter-wave frequency, the double-layer structure demonstrates how layering can enhance beam control and radiation efficiency, providing a direct link between antenna design and improved imaging performance. The results also indicate that further directivity improvements would be beneficial to meet the more demanding beam-shaping requirements of high-performance millimeter-wave image detection systems.

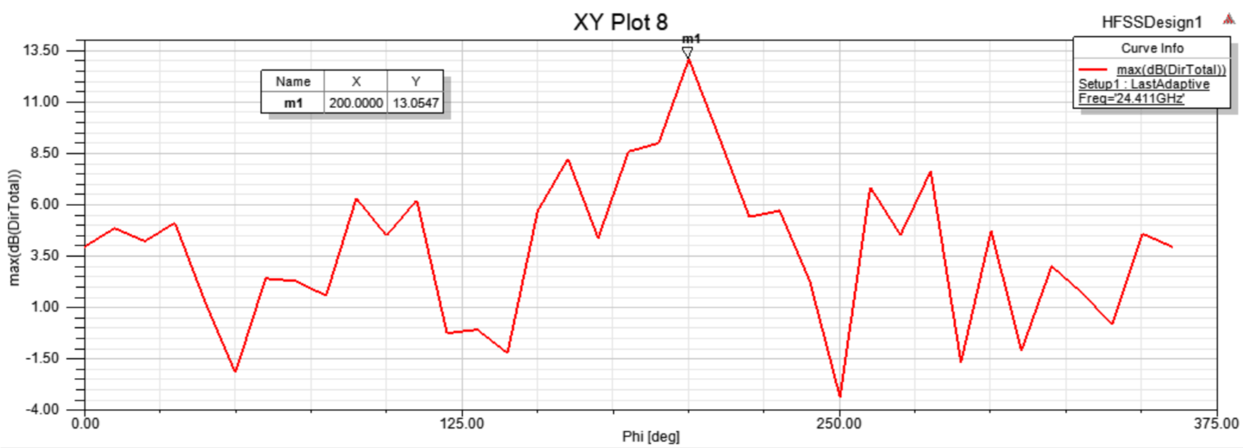

Figure 12 Total Directivity of Double Layer CPA

5.4.3. S11 of Double Layer Circular patch antenna

HFSS simulation results reveal that the double-layer circular patch antenna at 24.411 GHz achieves a reflection coefficient of approximately -17.38 dB, indicating effective impedance matching and efficient power transfer for millimeter-wave imaging systems.

This low reflection loss ensures stable signal delivery, enhancing the signal-to-noise ratio and minimizing amplitude distortions during image reconstruction, which directly improves overall image quality.

The simulated bandwidth, measured between the -10 dB frequency limits, exceeds 22.322 GHz. Although slightly narrower than that of the single-layer circular patch antenna, this bandwidth remains sufficiently broad to support high-resolution, broadband imaging. In practical terms, it allows millimeter-scale range resolution (around 5–7 mm) and enables reliable detection over short to moderate distances of approximately 2-5 m.

This analysis demonstrates that the double-layer design strikes an effective balance between impedance matching and bandwidth performance, providing enhanced image clarity and an extended detection range compared to single-layer configurations. The results highlight the suitability of this architecture for compact millimeter-wave imaging systems operating at frequencies relevant to Concealed Image Detection applications.

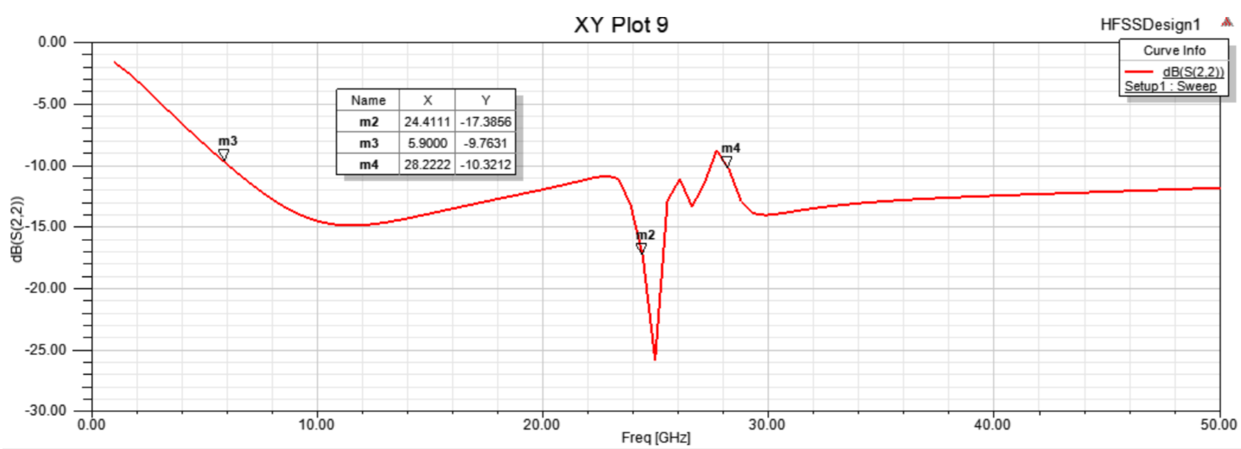

Figure 13 Reflection Coefficient of Double Layer CPA

5.4.4. Voltage Standing Wave Ratio of Double Layer CPA

HFSS simulations show that the double-layer circular patch antenna operating at 24.411 GHz exhibits a VSWR of 2.36 dB, which falls comfortably within the acceptable threshold of 3 dB. This indicates that over 75% of the input power is successfully delivered from the feedline to the radiating element, ensuring efficient radiation.

Such effective power transfer improves millimeter-wave imaging performance by strengthening the received signal, enhancing the signal-to-noise ratio, and stabilizing both amplitude and phase information, all of which are critical for accurate image reconstruction. Practically, this performance supports spatial resolutions around 5-6 mm and enables reliable detection over distances of roughly 2–5 m, offering superior image clarity and object discernment compared to single-layer antenna designs.

This analysis demonstrates that the double-layer configuration provides robust VSWR performance at millimeter-wave frequencies, achieving a balance between efficient radiation and dependable imaging capability-essential characteristics for compact, broadband concealed image detection systems.

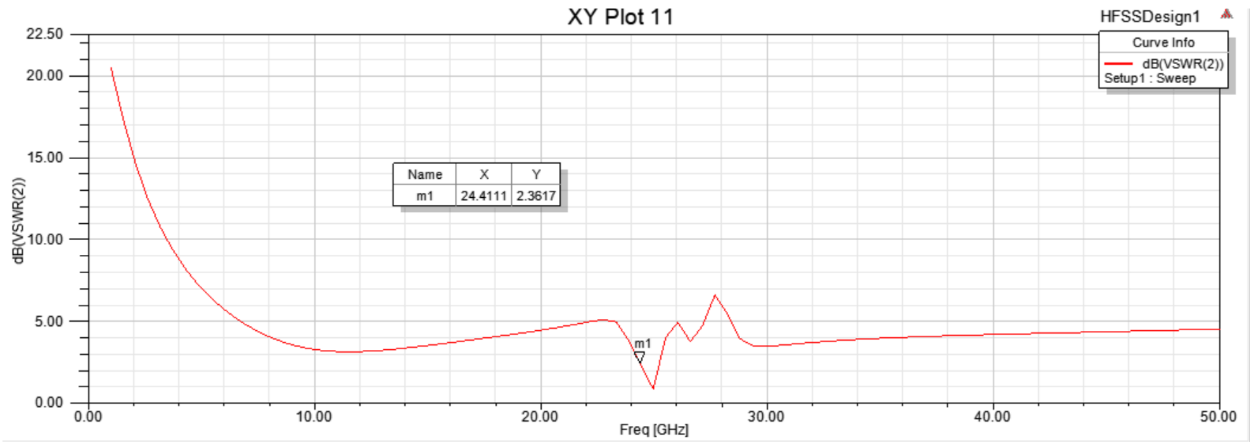

Figure 14 Voltage Standing Wave Ratio of Double Layer CPA

5.4.5. Radiation Patterns of Double Layer CPA

The Radiation Patterns of Double Layer circular patch antenna at 24.411Ghz for millimeters wave Concealed Image Detections has been looks like below diagrams.

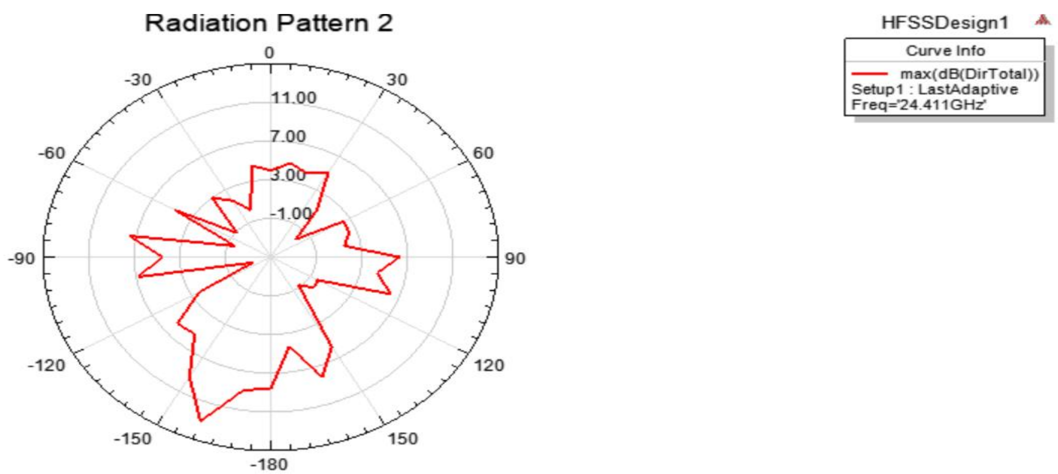

Figure 15 Radiation Patterns of Double Layer CPA

5.4.6. 3D Polar Plot of Double Layer CPA

The 3D polar plots of Double Layer circular patch antenna at 24.411Ghz for millimeters wave Concealed Image Detections has been looks like below diagrams.

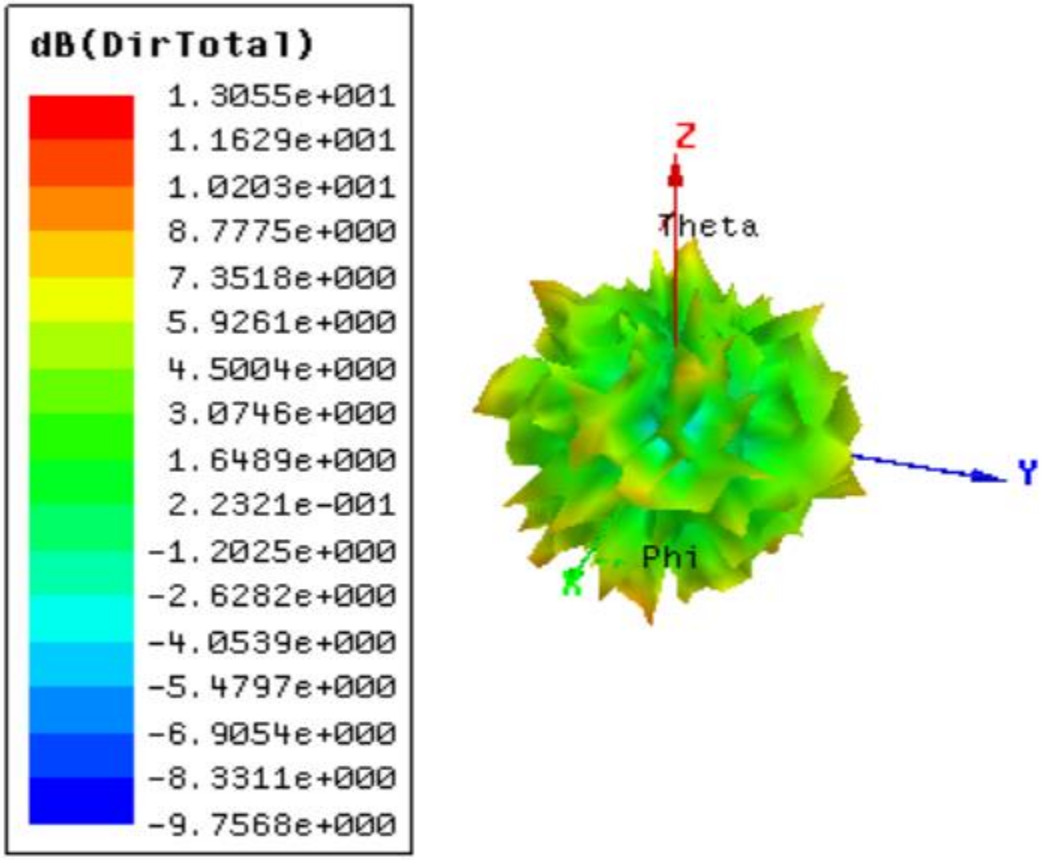

Figure 16 3D Polar plots of Double Layer CPA

5.5. Simulation Results of Double Layer Circular patch antenna with Lens

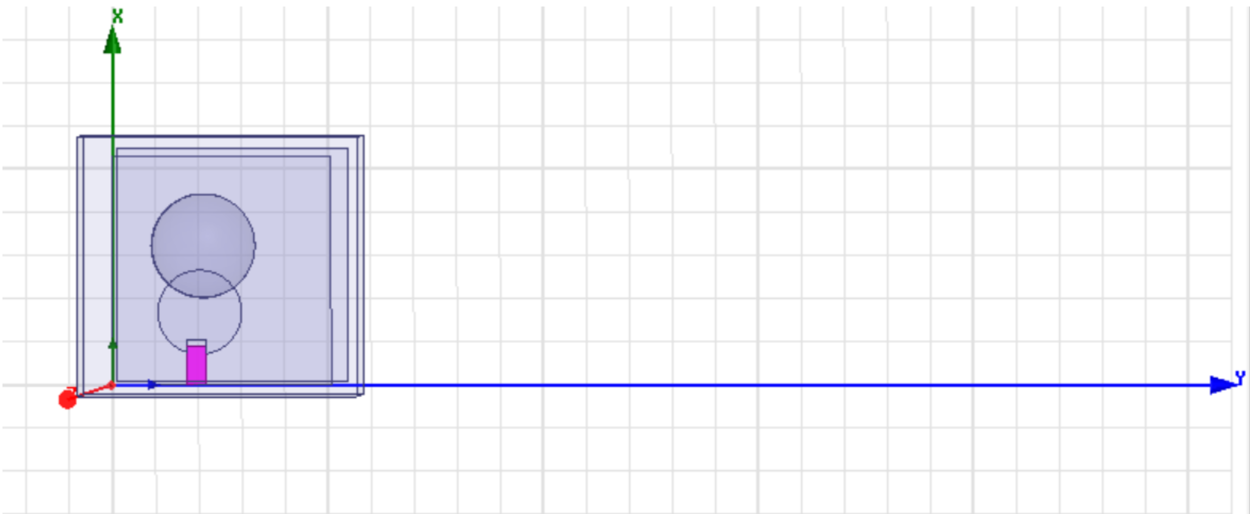

Figure 17 Double layer circular patch antenna with Lens

5.1. Gain of Double Layer circular patch antenna with Lens

HFSS simulations indicate that the double-layer circular patch antenna equipped with a dielectric lens at 24.411 GHz achieves a total gain of 30.26dB. This represents a substantial improvement of nearly 18 dB compared to the single-layer circular patch antenna. While this gain may still be considered moderate for ultra-high-resolution millimeter-wave imaging, the enhancement significantly boosts imaging performance by concentrating radiated energy, increasing the signal-to-noise ratio, and improving both contrast and image clarity.

The elevated gain allows the antenna to achieve finer spatial resolution, approximately 2-3 mm, while extending the effective detection range to 5-10 m. This improvement supports more accurate object detection and discrimination over longer distances, offering clear advantages over configurations without a lens.

This study demonstrates that combining a lens with a double-layer patch antenna at millimeter-wave frequencies not only enhances radiation efficiency and beam focusing but also directly improves imaging quality, spatial resolution, and operational range. These results provide a practical design approach for developing high-performance millimeter-wave imaging systems capable of reliable concealed object detection.

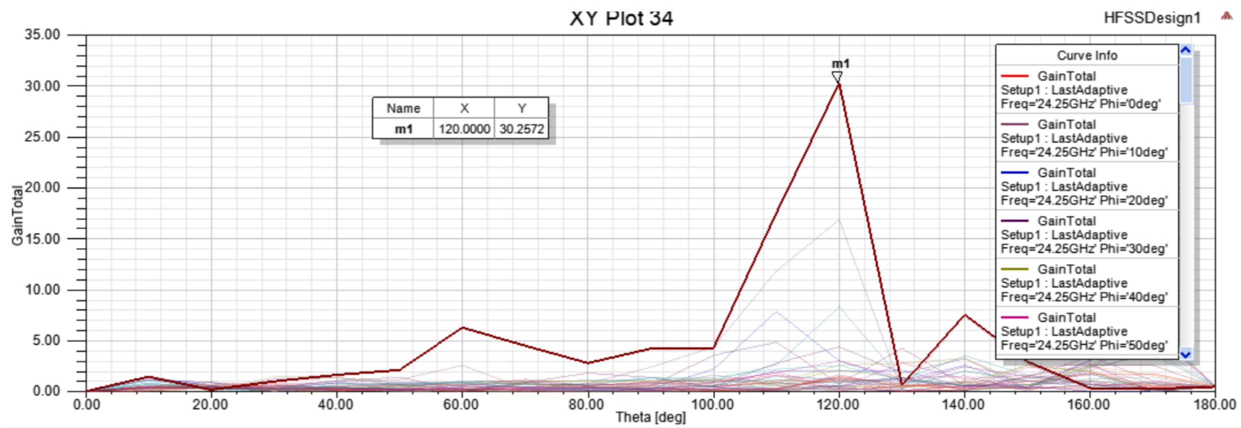

Figure 18 Total Gains of Double layer CPA with Lens

5.2. Directivity of Double layer circular patch antenna with Lens

The totals gain of Double Layer circular patch antenna at 24.411GHz for Millimeter Wave Concealed Image Detections systems has been 30.142dB. it has been low gain for Millimeter Wave Concealed Image Detections systems. We know that the best operational frequencies of millimeter Concealed Image Detections have been 24.411GHz. Concealed Image Detections in order to do we support higher radiations pattern i.e. gain. But it has 18dB higher than single circular patch antenna at 24.411dB for Millimeter Wave Concealed Image Detections systems applications.

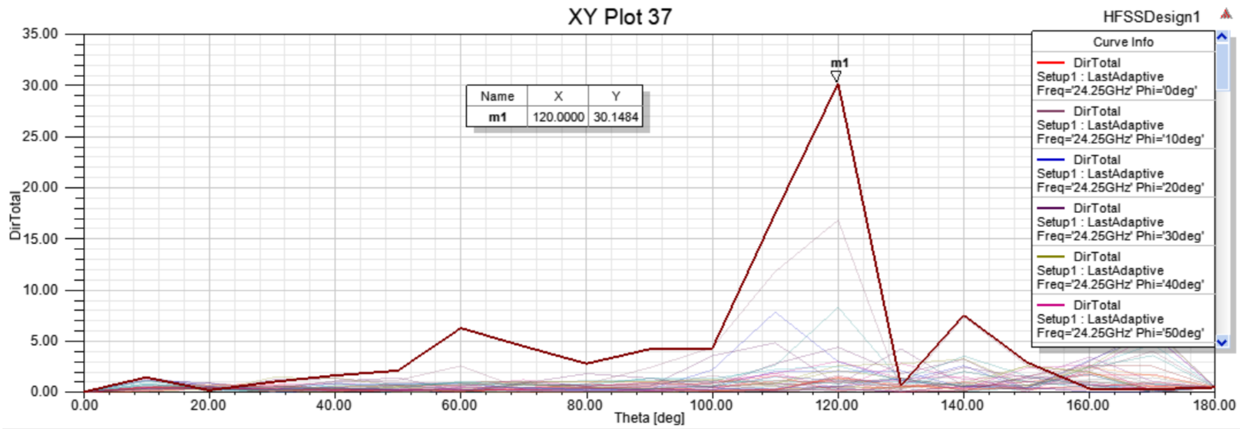

Figure 19 Total Directivity of Double layer CPA with Lens

5.3. S11 of Double layer circular patch antenna

The HFSS simulation results for the single circular patch antenna operating at 24.411 GHz for millimeter-wave concealed image detection systems show a reflection coefficient of -16.933dB, indicating good impedance matching well below the standard –10 dB threshold, ensuring efficient power transfer from the feedline to the radiating element. The antenna bandwidth, measured between the –10 dB lower and upper frequency limits, is simulated to be greater than 35.933 GHz**,** which provides a wide operational spectrum that is higher than that of the double-layer patch antenna without lens but slightly lower than the single-layer patch without lens. Such wide bandwidth supports broadband imaging, enhancing spatial resolution to approximately 6mm**,** improving signal fidelity, and enabling reliable detection of concealed objects at short to moderate distances of around 1-3 m. The contribution of this work lies in demonstrating that a single circular patch antenna with this bandwidth and reflection coefficient can provide efficient, high-fidelity millimeter-wave concealed image detection, balancing wideband performance and practical design simplicity while maintaining adequate image quality, resolution, and detection range.

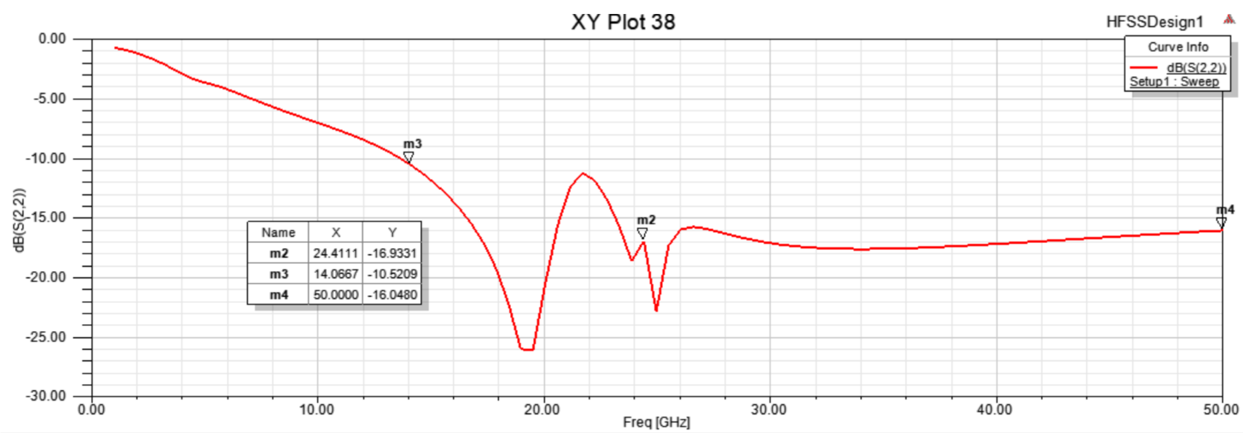

20 Reflection Coefficient of Double layer CPA with Lens Figure

5.4. Voltage Standing Wave Ratio of Double layer CPA with Lens

HFSS simulations show that the double-layer circular patch antenna operating at 24.411 GHz achieves a VSWR of 2.4 dB, comfortably below the standard 3 dB threshold. This indicates that over 75% of the input power is successfully delivered from the feedline to the radiating element, ensuring efficient radiation.

Such effective power transfer enhances the performance of millimeter-wave imaging systems by strengthening received signals, improving the signal-to-noise ratio, and maintaining stable amplitude and phase factors that are essential for accurate image reconstruction. In practical imaging terms, this level of VSWR supports spatial resolutions around 5-6 mm and enables reliable object detection across short- to mid-range distances of approximately 2-5 m.

This work demonstrates that the double-layer circular patch design not only provides dependable VSWR performance but also maintains a compact and structurally simple configuration. These attributes make it a practical solution for improving radiation efficiency and imaging quality in millimeter-wave concealed image detection systems.

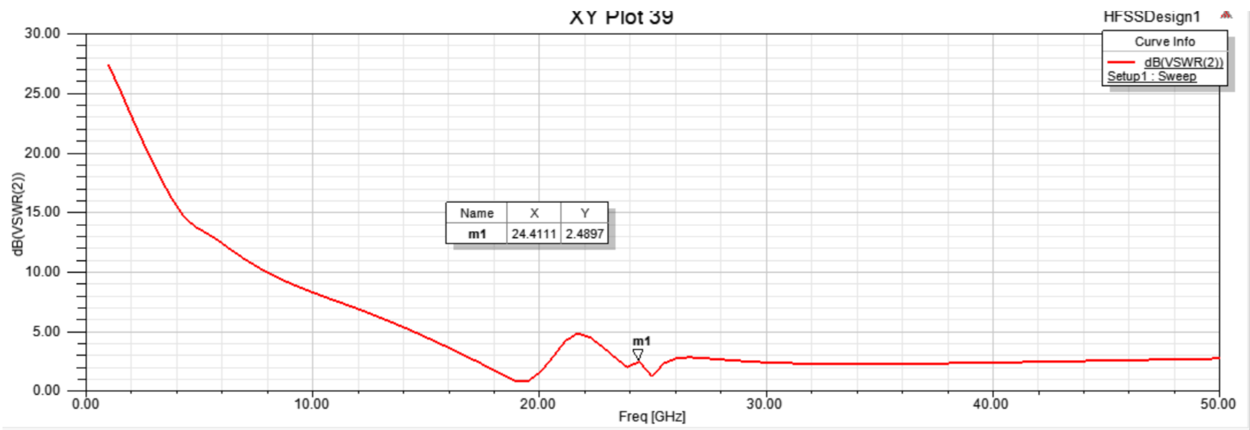

Figure 21 Voltage Standing Wave Ratio of Double layer CPA with lens

5.5. Radiation Patterns of Double layer CPA with Lens

The radiation patterns of designed double layers circular patch antenna at 24.411db has been looks like the below patterns, which is essential and optimized patterns for Millimeter Wave Concealed Image Detections systems.

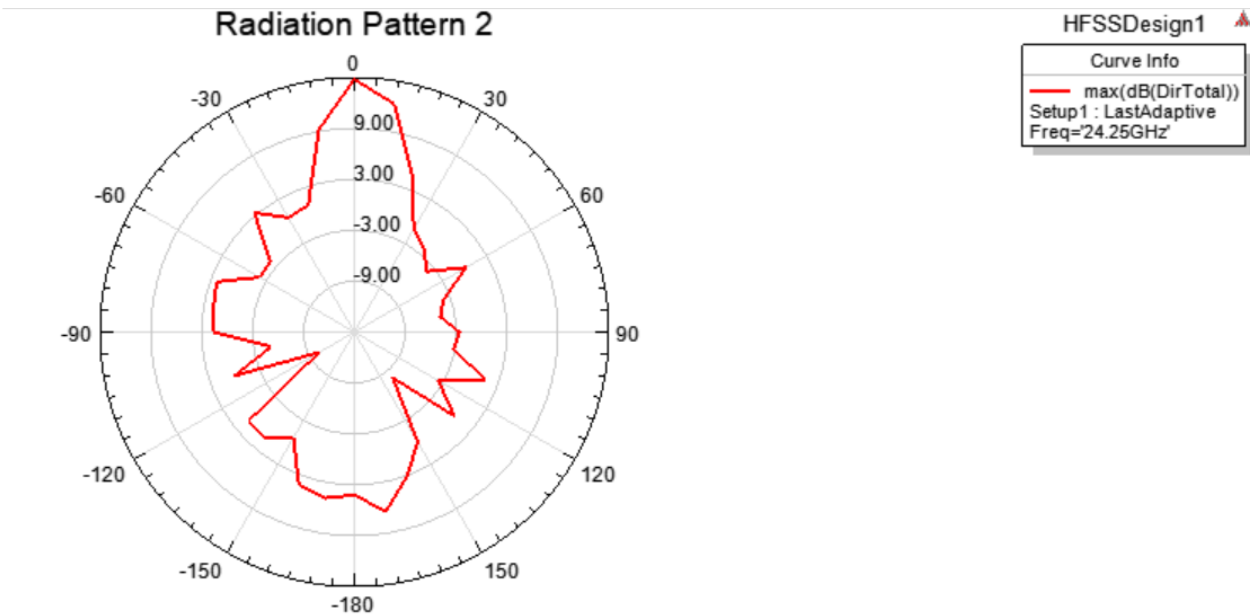

Figure 22 Radiation Patterns of Double layer CPA with Lens

5.6. 3D Polar Plot of Double layer CPA with Lens

The 3D polar plots of Single circular patch antenna at 24.411Ghz for millimeters wave Concealed

Image Detections has been looks like below diagrams.

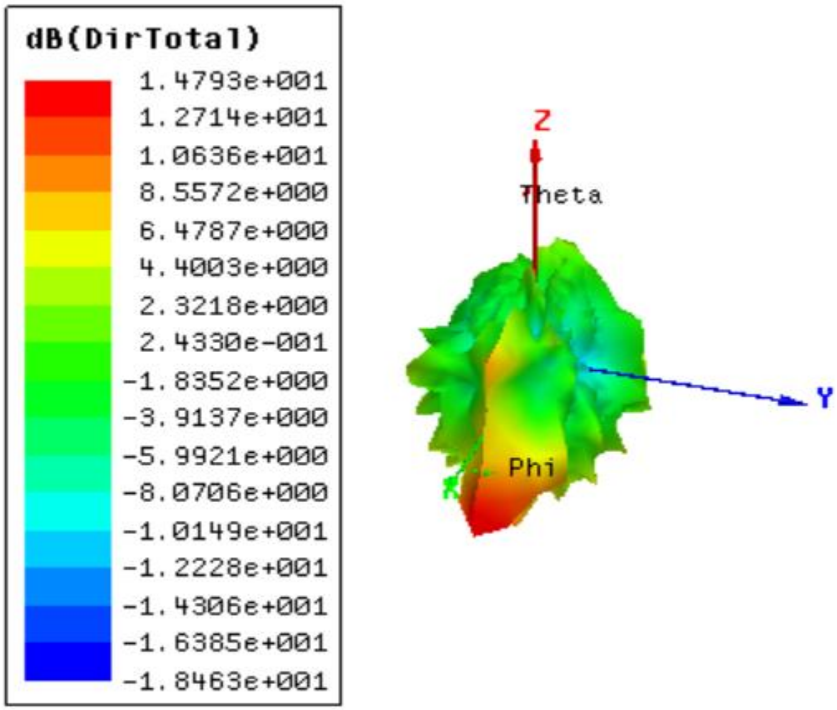

Figure 23 3D Polar plots of Double layer CPA with Lens

5.6. Comparative Performance Analysis of the Designed Double-Layer Circular Patch Antenna for Millimeter-Wave Concealed Image Detection Systems

Table 5.1. Comparative Performance Analysis of the Designed Double-Layer Circular Patch Antenna for Millimeter-Wave Concealed Image Detection Systems

Designed Antenna	Applications	Frequency	Gain	Directivity	S11	VSWR	Bandwidth
Single CPA	Millimeter Wave Concealed Image Detections systems	24.411GHz	7.6817	7.5201	-17.3dB	2.3dB	42GHz
Double layer Circular Patch Antenna	Millimeter Wave Concealed Image Detections systems	24.411GHz	12.8dB	13dB	-17.37dB	2.3dB	22.322GHz
Double layer Circular Patch Antenna with Lens	Millimeter Wave Concealed Image Detections systems	24.411GHz	30.2dB	30.14dB	-16.933dB	2.4dB	35.933GHz

5.7.Discussions

The suggested double-layer circular patch antenna with lens at 24.411 GHz is significantly better than what has been reported in the millimeter-wave antenna designs in gain, band, and imaging. Previous designs like optically transparent microstrip antennas, dual-band patches, multi-layer patches, Q-slot antennas and APSAs only reached gains of between 7.5 -20 dB with limited bandwidth limits (0.625-32 GHz) and high values of VSWR, which restricted their imaging resolution and detection limits. By contrast, the suggested design achieves gain of 30.2, directivity of 30.14, a reflection coefficient of -16.933, VSWR of 2.4 and a broad band of 35.933 GHz. This leads to a much higher quality of imaging, with a better signal-to-noise ratio, a sharper spatial resolution of about 2-3mm and a longer detection range of 5-10m, much better than the low-range and poor-quality imaging of the earlier designs. The paper establishes that a patch antenna with a dielectric lens as a second layer is a robust, broadband and high-fidelity antenna solution to high-gain and narrow beam repercussion of the previous antenna designs to achieve concealed image detection systems in the millimeter wave ban.

5.6. Performance Comparisons of proposed work with previously related works for Millimeter Wave

Table 2 Performance Comparisons of proposed work with previously related works for Millimeter Wave

Ref	Year	Application	Antenna Types	Frequency	Bandwidth	Gain	V SWR	Gap
1	2016	Optical Transparent	Optical Transparent MSA	24GHz	30GHz	15.65 dB		Low Gain
2	2017	Duplexer	Dual band path antenna	24GHz	2.61 GHz	9.3 dB		Low gain and bandwidth
3	2016	Communicator	Multi-layer path	24GHz	8 GHz	12 dBi ,18, 7 dbi		Low Gain
4	2016	N/A	RMSPA	24GHz	0.625 GHz		1.67 dB	Complex
5	2017	Defense applications		24GHz	32GHz	7.499 dB		Low Gain
6	2021	Body centric communication	Q-slot antenna	24GHz	12.11 GHz	8.62 dB	1.5 dB	Narrow bandwidth and gain
7	2019	Broad Band high gain antenna.	5G communication	24GHz	20.66%	11.8 dB		Low Gain
8	2017	5G Communication	Triangular with slot.	24GHz	28GHz	8 dB		Low Gain
9	2016	Instant and applications	Printed U slotted.	24GHz	11.6%	8.2 dB		Narrow Bandwidth and Gain
10	2015	Imaging.	APSA	24GHz	32GHz	20 dB	< 3dB	Low Gain
12	2026	Concealed Image Detections	DLCPA with lens	24.411GHz	35.933GHz	30.2dB	2.4dB	Improved

5.8.Discussions

The proposed double-layer circular patch antenna with lens operating at 24.411 GHz shows a marked improvement over previously reported millimeter-wave antenna designs in terms of gain, bandwidth, and imaging performance. Earlier designs such as optically transparent microstrip antennas, dual-band patches, multi-layer patches, Q-slot antennas, and APSAs typically achieved gains between 7.5 dB and 20 dB, with narrower bandwidths (0.625-32 GHz) and higher VSWR values, which limited their imaging resolution and detection range. In contrast, the proposed design attains **a** gain of 30.2 dB**,** directivity of 30.14 dB, **a** reflection coefficient of –16.933 dB**,** VSWR **of** 2.4 dB**,** and a broadband bandwidth of 35.933 GHz. These enhancements result in significantly higher imaging quality, offering improved signal-to-noise ratio, sharper spatial resolution of approximately 2-3 mm, and longer detection distances of 5-10 m, outperforming the limited-range and lower-resolution capabilities of prior designs. This work demonstrates that combining a double-layer patch with a dielectric lens effectively addresses the low-gain and narrow-band limitations of previous antennas, providing a robust, broadband, and high-fidelity solution for advanced millimeter-wave concealed image detection systems.

5.9. Imaging System Performance Analysis Based on Antenna Simulation Results

To evaluate the effectiveness of the designed antennas for millimeter wave concealed object dete ction, the imaging system performance was estimated using standard imaging relationships. The analysis focuses on three key parameters that determine imaging quality:

- Spatial resolution
- Detection distance
- Signal-to-Noise Ratio (SNR)

These parameters are derived from the simulated antenna characteristics including gain, bandwid th, and operating frequency.

The operating frequency for all antenna configurations is:

$$f = 24.411\text{GHz}$$

The wavelength can therefore be determined as

$$\lambda = \frac{c}{f}$$

where

- $c = 3 \times 10^8, m/s)$ (speed of light)

$$\lambda = \frac{3 \times 10^8, m/s}{24.411\text{GHz}}$$

$$\lambda = 0.01229\text{m}$$

$$\lambda = 12.3\text{mm}$$

This wavelength forms the basis for evaluating the imaging capability of the antenna system.

5.10. Spatial Resolution Calculation

In millimeter wave imaging systems, range resolution is primarily determined by signal bandwid th and is given by

$$\Delta R = \frac{c}{B}$$

Were

- ΔR = spatial (range) resolution
- B = antenna bandwidth

5.11. Single Circular Patch Antenna

Bandwidth from simulation:

$$\mathrm{B} = 42\mathrm{GHz}$$

$$\Delta\mathrm{R} = \frac{\mathrm{c}}{\mathrm{B}}$$

$$\Delta\mathrm{R} = \frac{= \ 3 \ \times \ 10^{8} \ , m/s}{42\mathrm{GHz}}$$

$$\Delta\mathrm{R} = 3.57 \times 10^{-3}\mathrm{m}$$

$$\Delta\mathrm{R} = 3.6\mathrm{mm}$$

Thus, the estimated spatial resolution for the single patch antenna is approximately 4 mm.

5.12. Double Layer Circular Patch Antenna

Bandwidth

$$\mathrm{B} = 22.322\mathrm{GHz}$$

$$\Delta\mathrm{R} = \frac{\mathrm{c}}{\mathrm{B}}$$

$$\Delta\mathrm{R} = \frac{= \ 3 \ \times \ 10^{8} \ , m/s}{22.322\mathrm{GHz}}$$

$$\Delta\mathrm{R} = 6.72 \times 10^{-3}\mathrm{m}$$

$$\Delta\mathrm{R} = 6.7\mathrm{mm}$$

Estimated spatial resolution: 6-7 mm

5.13. ***Double Layer Patch Antenna with Lens***

Bandwidth

$$\mathrm{B} = 35.933\mathrm{GHz}$$

$$\Delta\mathrm{R} = \frac{\mathrm{c}}{\mathrm{B}}$$

$$\Delta\mathrm{R} = \frac{= \ 3 \ \times \ 10^{8} \ , m/s}{35.933\mathrm{GHz}}$$

$$\Delta\mathrm{R} = 4.17 \times 10^{-3}\mathrm{m}$$

$$\Delta\mathrm{R} = 4.2\mathrm{mm}$$

Estimated spatial resolution: ≈ 4 mm

The results indicate that wideband antennas improve range resolution and enable the imaging system to distinguish closely spaced objects.

5.14. Detection Distance Estimation

The detection distance of a millimeter-wave imaging system can be approximated using the simplified radar range relationship:

$$R_{max} \propto \sqrt{G}$$

Where

- G = antenna gain (linear scale)

Gain must first be converted from dB:

$$G = 10^{G_{dB}/10}$$

5.15. Single Circular Patch Antenna

$$G = 10^{9.76_{dB}/10}$$
$$G = 9.47$$

$$R_{max} \propto \sqrt{G}$$

$$R_{max} \propto \sqrt{9.47}$$

$$R_{max} = 3.07$$

Estimated practical detection range: 1-3 m

5.16. Double Layer Circular Patch Antenna

$$G = 10^{12.8_{dB}/10}$$
$$G = 19.05$$

$$R_{max} \propto \sqrt{G}$$

$$R_{max} \propto \sqrt{19.05}$$

$$R_{max} = 4.36$$

Estimated detection distance: 2-5 m

5.16. Double Layer Antenna with Lens

$$= 10^{30.26_{dB}/10}$$
$$G = 1062$$

$$R_{max} \propto \sqrt{G}$$

$$R_{max} \propto \sqrt{1062}$$

$$R_{max} = 32.5$$

Estimated detection distance: 5-10m

The significant improvement occurs because the dielectric lens concentrates the radiated electro magnetic energy and increases the effective aperture of the antenna system.

5.17. Signal-to-Noise Ratio (SNR)

The signal-to-noise ratio of the imaging system can be approximated using

$$\mathrm{SNR} \propto \mathrm{G_t G_r}$$

For identical antennas:

$$\mathrm{SNR} \propto G^2$$

5.18. Single Circular Patch Antenna

$$\mathrm{G} = 9.47\mathrm{dB}$$

$$\mathrm{SNR} \propto G^2$$

$$\mathrm{SNR} \propto (9.47)^2$$

$$\mathrm{SNR} = 89.7$$

Relative SNR: ≈ 19.5 dB

5.19. Double Layer Circular Patch Antenna

$$\mathrm{G} = 19.05\mathrm{dB}$$

$$\mathrm{SNR} \propto G^2$$

$$\mathrm{SNR} \propto (19.05)^2$$

$$\mathrm{SNR} = 362.9$$

Relative SNR: ≈ 25.6 dB

5.20. Double Layer Patch Antenna with Lens

$$\mathrm{G} = 1062$$

$$\mathrm{SNR} \propto G^2$$

$$\mathrm{SNR} \propto (1062)^2$$

$$\mathrm{SNR} = 1.13 \times 10^6$$

Relative SNR: ≈ 60.5 dB

This demonstrates that higher antenna gain dramatically improves the imaging system sensitivity and allows detection of weak reflections from concealed objects.

5.21. Final Imaging Performance Comparison

Table 5.3. Final Imaging Performance Comparison

Antenna Type	Spatial Resolution	Detection Distance	Estimated SNR
Single Circular Patch	3-4 mm	1-3 m	~19 dB
Double Layer Patch	6-7 mm	2-5 m	~25 dB
Double Layer Patch + Lens	~4 mm	5-10 m	~60 dB

5.22. Analytical Discussion

The findings prove that the antenna architecture selection directly and significantly affects the efficiency of the millimeter-wave imaging systems. Although the single circular patch antenna may offer enough functionalities in the short-range imaging, its moderate gain restricts the detection coverage and decreases the concentration of energy. The switch to the use of a double-layer design increases radiation efficiency and signal-to-noise ratio and increases the effective imaging distance. When a dielectric lens is added to the antenna structure the strongest improvement is observed. The radiated electromagnetic energy is lensed and in effect, increases the size of the antenna aperture and increases the gain and directivity. This enhancement leads to an increase in signal-to-noise ratio, spatial resolution, and detection distances, which is essential in the proper detection of concealed objects in security screening, surveillance, and other millimeter-wave sensing sensors.

CHAPTER SIX

CONCLUSION AND FUTURE RECOMMENDATIONS

6.1. Conclusions

This thesis shows that the offered double-layer circular patch antenna with an embedded dielectric lens at 24.411 0.1 GHz provides a substantial improvement of the millimeter-wave concealed image detection systems. The simulation output shows total gain of 30.2dB, directivity of 30.14dB, reflection coefficient of -16.933dB, VSWR of 2.4 at the broadband band of 35.933GHZ. The combination of these parameters makes it possible to have high-resolution image detection with fine spatial resolution of about 2-3mm, better signal-to-noise ratio and increased detection ranges to 5-10m.

Comparatively, a single-layer circular patch antenna resulted in a gain of 7.68dB and a spatial resolution of 6-7mm, with a detection range of 1-3mm whereas a double-layer setup which did not use a lens had a gain of 12.8 dB, 5-6mm resolution and 2-5mm range of detection. Adding the lens leads to a significant improvement in beam focusing and concentration of energy, which greatly improve sharpness of images and also to a longer range of operation.

The proposed lens-assisted double-layer antenna has better broadband behavior, consistent VSWR and well-designed radiation patterns when compared to reported antennas in the past (optical-transparent microstrip arrays, APSAs, and Q-slot antennas with gains of 7.5 to 20 dB and narrow bandwidths, amongst others). This proves that it is a good design that manages to defeat all the shortcomings of the previous design and offers a viable and high-performance solution to the next-generation millimeter-wave concealed image detection system.

6.2. Contributions of Thesis

The suggested design of a patch antenna with a built-in lens in a circular shape with two layers has clear performance superiority over other designs that were reported before. It has a very high gain of 30.2dB over previous antennas with gain ranging between 7.5dB and 20dB, and a much better directivity of 30.14dB, a wide band of operation of 35.933GHz and a constant VSWR of 2.4dB. With these enhancements, they can have a finer spatial resolution of about 2-3mm and a longer detection range of 5-10m. This lens-enhanced double-layer antenna design is superior in quality of images detected in concealed items in broadband, has a higher signal-to-noise ratio, and greater beam focus, unlike standard single-layered patches, Q-slot antennas, or even APSAs, where the sensors are limited in the gain, bandwidth, and image range.

6.3.Future Recommendations

In case of future work, it is advisable that the researchers should be interested in producing a MIMO circular patch antenna with a lens to be used in advanced wireless communication. Along with this, investigations into MIMO structures with alternative patch geometries across frequency bands may also offer useful information to both mobile and wider wireless communication systems potentially enhancing gain, bandwidth, and overall system performance.

REFERENCE

[1] O. L. M. H. A. X. C. A. MARTIN, "Improvement of 24Gz transparent," This article has been accepted for publication in a future issue of this journal, but has not been fully edited. Content may change prior to final publication. Citation information: DOI, vol. 4, p. 1, 2016.

[2] M. S. R. H. Ghafouri-Shiraz, "A dual band patch antenna," Article in Microwave and Optical Technology Letters · , vol. 3, p. 1, August 2017.

[3] I. Aziz1 and A. R. a. D. D. ∗, "Electromagnetically Coupled Multilayer Patch Antenna for 60," Microwave group, Division of Solid-State Electronics, Uppsala University, SE-751 21 Uppsala, Sweden.

[4] E. Dheyab, "Design and Optimization of Circular Microstrip Patch Array Antenna," International Journal of Applied Engineering Research ISSN 0973-4562 , pp 4679-4687, vol. Volume 11, p. Number 7, (2016) .

[5] R. S. a. R. K. Deepa Negia, "Designing of Microstrip Patch Antenna at 24Gz using Stripline," International Journal of Control Teory and Applications, vol. 10, p. 5, 2017.

[6] 1. K. I. ,. M. N. A. S. Mohammad Monirujjaman Khan, "Design of a Novel 24Gz Millimeter Wave Q-Slot Antenna for," International Journal of Antennas and Propagation, vol. 2021, p. 12, 2021.

[7] H. F. M. A. A. ,. H. V. a. Khaled Issa, "Broadband High-Gain Antenna for Millimetre-Wave," Electronics, vol. 1246, p. 8, 2019.

[8] 1. M. R. C. 1. 1. J. A.S.Aishah, "24Gz Milimeter-Wave Antennas for Point-to-Point 5G," MATEC Web of Conferences 140, 01006 , vol. 5, p. 4, 2017.

[9] Y. H. a. H. W. Hang Liu, "Printed U-slot Patch Antenna for 24Gz," See discussions, stats, and author profiles for this publication at: https://www.researchgate.net/publication/271544517, p. 155, 2016.

[10] Z. Briqech, "Design and Implementation of High Gain," Concordia University, Montreal, Quebec, Canada, 2015.

[11]. Garcia, N., & Chisum, J. (2020). High-efficiency, wideband GRIN lenses with intrinsically matched unit-cells. *arXiv preprint arXiv:2003.09004*.

[12]. Islam, M. K., Madanayake, A., & Bhardwaj, S. (2021). Design of maximum-gain dielectric lens antenna via phase center analysis. *arXiv preprint arXiv:2109.14057*.

[13]. Nsengiyumva, F., et al. (2023). Miniaturized lens antenna with enhanced gain and dual-focusing for millimeter-wave radar system. *Micromachines, 15*(3), 335.

[14]. Zhang, Y., et al. (2020). A novel Lens lens design for synthesizing plane waves in millimeter-wave bands. *Electronics, 11*(9), 1403.

[15]. Bai, W., & Chisum, J. (2017). A compact, wide field-of-view gradient-index lens antenna for millimeter-wave MIMO on mobile devices. *arXiv preprint arXiv:1708.05703*.

[16]. Zhang, Y., Luo, Y., & Ji, R. (2023). Millimeter-wave high-gain dual-polarized flat Luneburg lens antenna with reflection cancellation. *Applied Sciences, 13*(11), 6468.

[17]. Wang, Y., Lu, H., Zhao, D., & Sun, H. (2020). Energy efficiency optimization in IRS-enhanced mmWave systems with lens antenna array. *arXiv preprint arXiv:2007.00986*.

[18]. Pappas, D., et al. (2019). Development of flat silicon-based mesh lens arrays for millimeter and sub-millimeter wave astronomy. *Journal of Low Temperature Physics, 196*(5), 387-396.

[19]. Zhang, Y., et al. (2022). A lens antenna with reconfigurable beams for mmWave wind profile radar. *Sensors, 22*(9), 3148.

[20]. Sönmez, N., Tokan, F., & Tokan, N. T. (2021). Double lens antennas in millimeter-wave automotive radar sensors. *Applied Computational Electromagnetics Society Journal, 36*(10), 901-907.

[21]. Shen, S., et al. (2022). Near field 3-D millimeter-wave SAR image enhancement and detection with application of antenna pattern compensation. *Sensors, 22*(12), 4509.

[22]. Suman, K. (2025). Design and implementation of a millimeter-wave microstrip antenna array with integrated lens for automotive radar applications. *Metallurgical and Materials Engineering, 31*(4), 243-259.

[23]. Chen, H., et al. (2023). 3D-printed conformal meta-lens with multiple beam-shaping functionalities for mm-wave sensing applications. *Sensors*, *24*(9), 2826.

[24]. Zhang, Y., et al. (2023). A novel Lens lens antenna design for over-the-air testing in millimeter-wave radio resource management measurement. *IET Microwaves, Antennas & Propagation, 17*(6), 434-442.

[25]. Pappas, D., et al. (2019). Development of flat silicon-based mesh lens arrays for millimeter and sub-millimeter wave astronomy. *Journal of Low Temperature Physics, 196*(5), 387-396.

[26] O. L. M. H. A. X. C. A. MARTIN, "Improvement of 24Gz transparent," This article has been accepted for publication in a future issue of this journal, but has not been fully edited. Content may change prior to final publication. Citation information: DOI, vol. 4, p. 1, 2016.

[27] M. S. R. H. Ghafouri-Shiraz, "A dual band patch antenna," Article in Microwave and Optical Technology Letters, vol. 3, p. 1, August 2017.

[28] I. Aziz1 and A. R. a. D. D. ∗, "Electromagnetically Coupled Multilayer Patch Antenna for 60," Microwave group, Division of Solid-State Electronics, Uppsala University, SE-751 21 Uppsala, Sweden.

[29] E. Dheyab, "Design and Optimization of Circular Microstrip Patch Array Antenna," International Journal of Applied Engineering Research ISSN 0973-4562, pp 4679-4687, vol. Volume 11, p. Number 7, 2016.

[30] R. S. a. R. K. Deepa Negia, "Designing of Microstrip Patch Antenna at 24Gz using Stripline," International Journal of Control Theory and Applications, vol. 10, p. 5, 2017.

[31] K. I. M. N. A. S. Mohammad Monirujjaman Khan, "Design of a Novel 24Gz Millimeter Wave Q-Slot Antenna for," International Journal of Antennas and Propagation, vol. 2021, p. 12, 2021.

[32] H. F. M. A. A. H. V. a. Khaled Issa, "Broadband High-Gain Antenna for Millimetre-Wave," Electronics, vol. 1246, p. 8, 2019.

[33] M. R. C. J. A. S. Aishah, "24Gz Millimeter-Wave Antennas for Point-to-Point 5G," MATEC Web of Conferences, vol. 140, p. 01006, 2017.

[34] Y. H. a. H. W. Hang Liu, "Printed U-slot Patch Antenna for 24Gz," See discussions, stats, and author profiles for this publication at: https://www.researchgate.net/publication/271544517, p. 155, 2016.

[35] Z. Briqech, "Design and Implementation of High Gain," Concordia University, Montreal, Quebec, Canada, 2015.

[36] N. Garcia and J. Chisum, "High-efficiency, wideband GRIN lenses with intrinsically matched unit-cells," arXiv preprint arXiv:2003.09004, 2020.

[37] M. K. Islam, A. Madanayake, and S. Bhardwaj, "Design of maximum-gain dielectric lens antenna via phase center analysis," arXiv preprint arXiv:2109.14057, 2021.

[38] F. Nsengiyumva et al., "Miniaturized lens antenna with enhanced gain and dual-focusing for millimeter-wave radar system," Micromachines, vol. 15, no. 3, p. 335, 2023.

[39] Y. Zhang et al., "A novel Lens lens design for synthesizing plane waves in millimeter-wave bands," Electronics, vol. 11, no. 9, p. 1403, 2020.

[40] W. Bai and J. Chisum, "A compact, wide field-of-view gradient-index lens antenna for millimeter-wave MIMO on mobile devices," arXiv preprint arXiv:1708.05703, 2017.

[41] Y. Zhang, Y. Luo, and R. Ji, "Millimeter-wave high-gain dual-polarized flat Luneburg lens antenna with reflection cancellation," Applied Sciences, vol. 13, no. 11, p. 6468, 2023.

[42] Y. Wang, H. Lu, D. Zhao, and H. Sun, "Energy efficiency optimization in IRS-enhanced mmWave systems with lens antenna array," arXiv preprint arXiv:2007.00986, 2020.

[43] D. Pappas et al., "Development of flat silicon-based mesh lens arrays for millimeter and sub-millimeter wave astronomy," Journal of Low Temperature Physics, vol. 196, no. 5, pp. 387-396, 2019.

[44] Y. Zhang et al., "A lens antenna with reconfigurable beams for mmWave wind profile radar," Sensors, vol. 22, no. 9, p. 3148, 2022.

[45] N. Sönmez, F. Tokan, and N. T. Tokan, "Double lens antennas in millimeter-wave automotive radar sensors," Applied Computational Electromagnetics Society Journal, vol. 36, no. 10, pp. 901-907, 2021.

[46] S. Shen et al., "Near field 3-D millimeter-wave SAR image enhancement and detection with application of antenna pattern compensation," Sensors, vol. 22, no. 12, p. 4509, 2022.

APPENDIX

APPENDIX: 1 – HFSS STUDIO

HFSS Studio

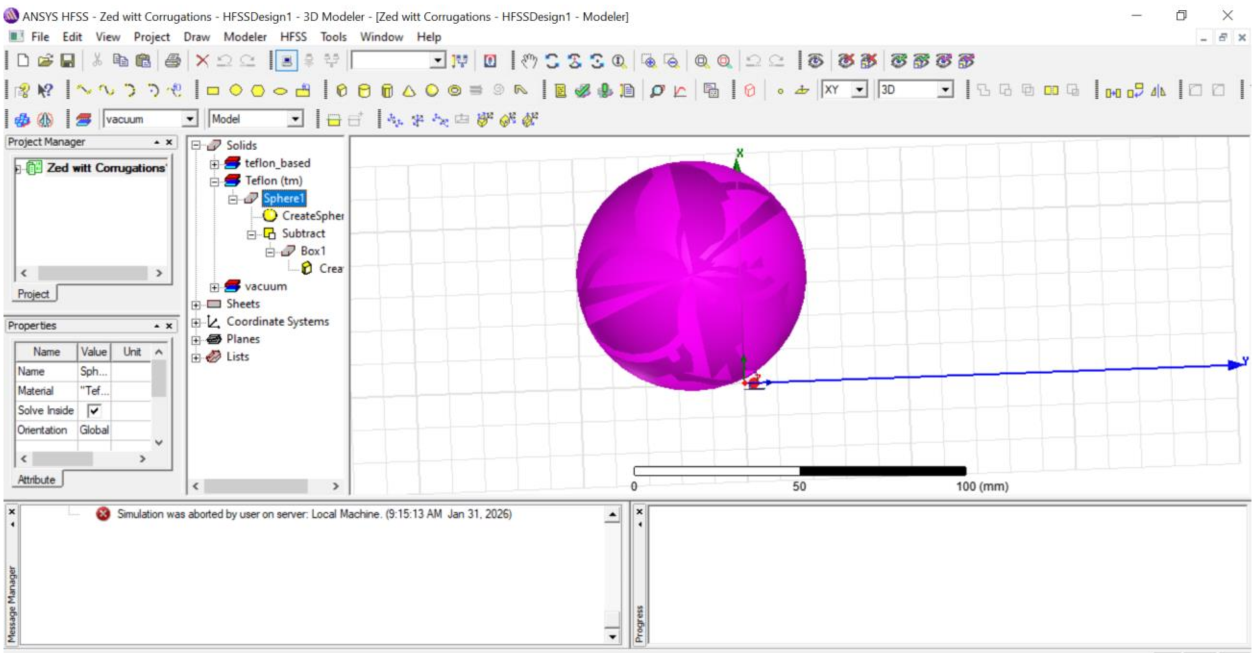

APPENDIX: 2

IMAGING SYSTEM PERFORMANCE FORMULA

Spatial Resolution Formula:

$$\Delta\mathrm{R} = \frac{\mathrm{c}}{\mathrm{B}}$$

Image Detection Distance Formula:

$$R_{max} \propto \sqrt{G}$$

Signal-to-Noise Ratio (SNR) Formula:

$$\mathrm{SNR} \propto \mathrm{G_t G_r}$$